

## Effect of iron(hydr)oxide formation on micropollutant removal in drinking water treatment

BTO 2020.059

**Datum**

30 mei 2020

**Opdrachtgever**

BTO Bronnen en Omgeving

**Meer informatie**

dr. ir. C.H.M. Hofman-Caris

T 0653198167

E roberta.hofman-caris@kwrwater.nl

**Auteurs**

Dr. ir. C.H.M. (Roberta) Hofman-Caris

Dr. B (Bas) van der Grift

**Opdrachtnummer**

402045-175

**Kwaliteitsborger**

Dr. B (Bas) van der Grift

**Projectmanager**

Martin van der Schans

**Pagina**

1/34

## Summary

Both in oxic and in anoxic water iron redox reactions can occur. During these reactions reactive components are formed, either via an oxidative or a reductive pathway, depending on conditions. According to the oxidative pathway Fenton-like processes may occur, in which sunlight and surfaces play a crucial role. During these cycling processes reactive compounds like  $\text{HO}\cdot$ ,  $\text{HO}_2\cdot$ ,  $\text{ROO}\cdot$ ,  $\text{Fe}^{2+}$  and  $\text{Fe}^{3+}$  are formed. Although they are present in low concentrations (order of magnitude ng/L), cycles may occur 30 times per hour. Apart from chemical and physical parameters, also biological processes may be involved in the reactions that occur because of iron redox cycling in surface water and produce reactive compounds.

According to the reductive pathway, which occurs in anoxic groundwater, electrons are the main reactive species, and here too surfaces play a crucial role.

All processes mentioned above may be involved in the degradation of organic micropollutants. However, very limited information is available on the actual role of iron redox cycling on the degradation of OMPs, both under oxic and anoxic circumstances. For the Dutch reservoirs, the possible effect of Fenton-like reactions on the degradation potential of OMPs was estimated, assuming a light penetration depth of about 10 cm. It showed that depending on the local circumstances, the degradation may vary between 0 and 100 %, which is in accordance with practical findings, although it is not known whether iron redox cycling actually plays a role in this. And the important question here is whether the degradation of OMPs can be improved by adding additional iron.

However, it was concluded that it certainly would be worthwhile to further investigate this possibility, and establish the role of Fenton-like reactions on OMP concentrations, how  $\text{FeCl}_3$  or  $\text{FeSO}_4$  dosing may affect the iron concentration in water and the light penetration depth of the water.

# Contents

<b>Summary</b>	<b>1</b>
<b>1 Introduction</b>	<b>3</b>
<b>2 Iron redox cycling</b>	<b>5</b>
2.1 Redox cycling and the removal of organic micropollutants	5
2.2 Oxidative pathway	5
2.2.1 Chemical redox reactions	5
2.2.2 Biologically induced redox cycling of iron	13
2.2.3 Degradation of organic micropollutants by (indirect) photolysis of surface waters	14
2.3 Reductive pathway	16
2.3.1 Chemical processes	16
2.3.2 Potential effect of subsurface iron removal	19
<b>3 OMP degradation potential</b>	<b>20</b>
3.1 The oxidative pathway	20
3.2 The reductive pathway	22
3.3 Research questions	23
<b>4 Conclusions</b>	<b>24</b>
<b>5 References</b>	<b>26</b>
<b>I Kinetic data for Fe redox cycling in literature</b>	<b>29</b>

## 1 Introduction

### 1.1 Problem indication

In the Netherlands about 65% of the drinking water is made from groundwater, and 35% from surface water. During drinking water treatment in all cases iron (hydr)oxides are formed, either at the surface or in the subsoil. For the removal of phosphate, particles and some organic matter, Fe(III) is added to surface water, sometimes in the reservoirs, sometimes during pretreatment of the water. The intake of drinking water utility Dunea is located in the “Afgedamde Maas”, a dead end side stream of the river Meuse. Here  $\text{FeSO}_4$  is added and the water is aerated.  $\text{Fe}^{3+}$  destabilizes particles, which results in coagulation and flocculation, during which process also natural organic matter may be incorporated into the growing flocs. After coagulation, flocculation and sedimentation the water of Dunea passes some microsieves, and is transported to Bergambacht, where dual media rapid sand filtration is applied, before the water is infiltrated into the dunes. Another Dutch drinking water utility, WML, doses  $\text{FeCl}_3$  to the reservoir “De Lange Vlieter” for the removal of phosphate, and Evides applies phosphate removal in reservoir I of Braakman. Also in the treatment of river bank filtrate or dune water iron is applied. Nearly all Dutch drinking water companies that use surface water as a source apply the coagulation/ flocculation/ sedimentation process adding Fe(III) (see Figure 1). However, internationally often also Al(III) can be used. In the Netherlands this only is done at production location “De Punt” of WBG, and at site Braakman of Evides.

Nearly all Dutch drinking water utilities that use groundwater as a source, apply deferrization either in the subsoil, or above ground during water treatment. During aeration Fe(II) is oxidized to Fe(III), which precipitates in a combination of ironhydroxides and ironoxides (see Figure 1). Here too, particles and organic material causing color and smell, are removed during coagulation/ flocculation/sedimentation.



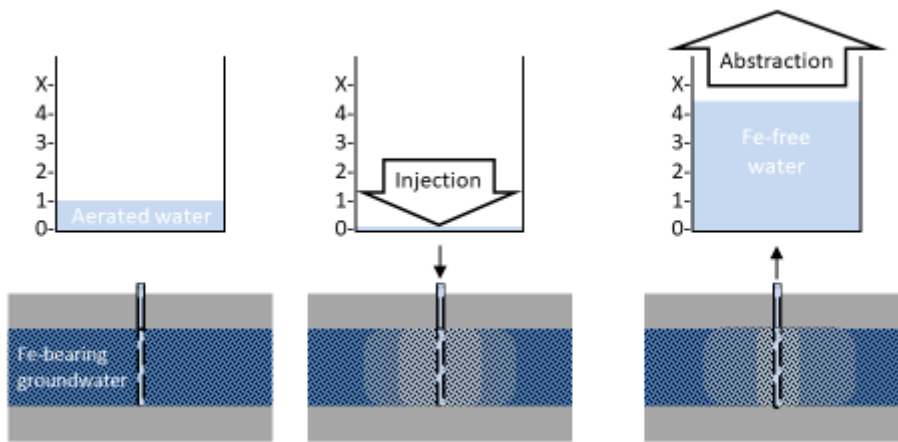


Figure 1: Examples of Iron application in drinking water production, aeration of groundwater for iron removal (left), and iron addition to surface water (right)

The iron redox processes occurring during water treatment may also contribute to the degradation of organic micropollutants. So far little attention has been paid to this possible contribution of iron redox cycling. In another project on Dutch reservoirs amongst others the degradation of organic micropollutants has been studied (Bertelkamp et al. 2020). In the reservoirs of PWN hardly any removal was observed, but in the reservoirs of Evides depending on e.g. seasonal variations  $\geq 90\%$  removal could be found for compounds like metoprolol, guanylurea, bisoprololol, AMPA (aminomethyl phosphonic acid), whereas for e.g. pyrene, (2-methyl thio) benzothiazole,, levetiracetam, iprodion, MTBE, uropropine, dyclofenac and DIPE (di-isopropyl ether) significant removal  $> 30\%$  was observed. It is not clear, however, whether and if yes how iron redox cycling may be involved in this.

## 1.2 Aim and outline

The aim of this report is to explore the possible contribution of redox cycling to degradation of organic micropollutants in Dutch and Flemish reservoirs with intake water and groundwater production wells.

Chapter 2 gives an overview of the findings from literature regarding iron redox cycling and organic micropollutant removal for two pathways of degradation. In chapter 3 we tried to estimate the OMP degradation potential of Fe redox cycling with some simple calculations. Chapter 4 gives the initial conclusions.

## 2 Iron redox cycling

### 2.1 Redox cycling and the removal of organic micropollutants

The presence of organic micropollutants in surface water, groundwater and sources for drinking water is increasingly becoming a matter of concern. Micropollutants like pharmaceuticals, pesticides, personal care products and industrial compounds have to be removed from water in order to be able to produce safe drinking water, but these compounds also affect aquatic life. A lot of research effort is made to address these problems, involving advanced technologies like reverse osmosis, advanced oxidation and adsorption onto various media. However, one type of processes, which always occurs during e.g. drinking water treatment, is the redox cycling of iron. The role this redox cycling might play in micropollutant removal from water so far has only attracted limited attention.

There are two possible pathways for contaminant degradation during this redox cycling:

1. Oxidation by reaction with reactive oxygen species (ROS) produced during redox cycling, like the photo-Fenton process
2. Reduction by electron transfer during heterogeneous oxidation of Fe(II) on surfaces of iron (hydr)oxide particles under anoxic conditions

Both pathways will be discussed in more detail in this report.

### 2.2 Oxidative pathway

#### 2.2.1 Chemical redox reactions

In the environment iron is subsequently oxidized and reduced, depending on the local bio-geochemical redox conditions. During these processes iron(hydr)oxide particles subsequently precipitate and dissolve. During these processes also Reactive Oxygen Species (ROS) are formed and degraded. Examples of ROS are the superoxide-anion radical  $O_2^{\cdot-}$ , hydrogen peroxide  $H_2O_2$  and the hydroxyl radical  $OH\cdot$ . ROS can be formed during oxidation of Fe(II) to Fe(III) by oxygen, and during reduction of Fe(III) with dissolved organic matter (DOC). These ROS can subsequently be involved in the oxidation of organic compounds including natural organic matter (like humic and fulvic acids) and organic contaminants. This redox cycling thus has environmental consequences beyond iron's role as a nutrient and as a sorbent (Voelker et al. 1997), catalyzing the degradation of dissolved organic matter.

Iron photo-redox cycling in lakes has been shown to catalyze the oxidation of dissolved organic matter (Voelker et al. 1997). This process may significantly reduce the concentrations of non-biodegradable material (i.e., humic substances) or organic micropollutants, as a result of the formation and reaction of transient species such as  $H_2O_2$ ,  $OH\cdot$ , and  $HO_2/O_2\cdot^-$ . Especially the highly reactive hydroxyl radical  $OH\cdot$  will non-selectively oxidize organic micropollutants in natural water (Southworth and Voelker 2003). The production of this reactive radical thus may contribute to the degradation of organic micro contaminants, although its effectiveness will depend on the concentration of both the hydroxyl radical and the water composition.

Redox cycling of iron in the presence of organic substances and light comprise a rather complex set of chemical reactions, that include both redox reactions of dissolved Fe species and reactions that take place on the surface of the iron oxide particles, as well as the transfer of iron species from the surface to the solution and vice versa (Voelker et al. 1997). These processes are summarized in Figure 2.

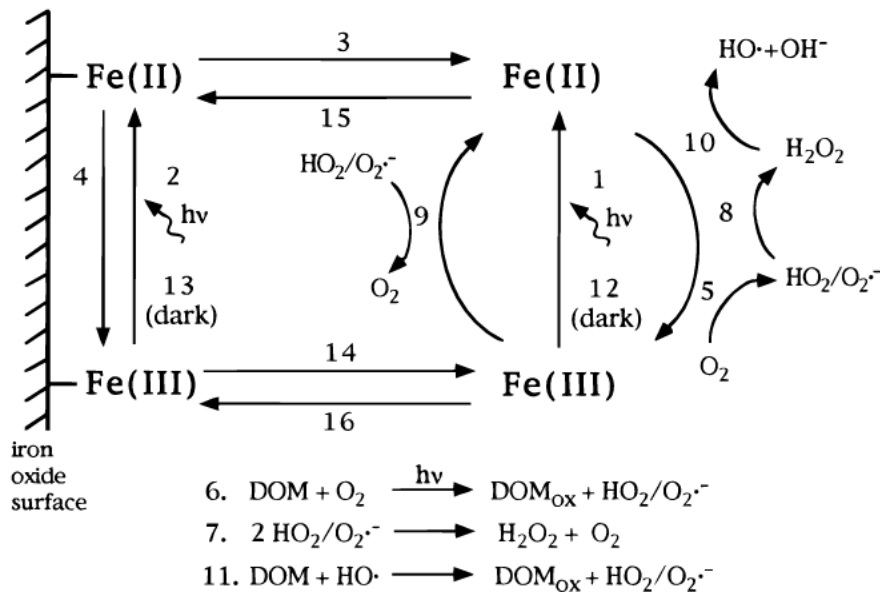


Figure 2.: Schematic summary of possible iron reactions in surface waters: (1) photo-reduction of dissolved Fe(III) by DOM, (2) photoreduction of surface Fe(III) by DOM, (3) detachment of surface Fe(II), (4) re-oxidation of surface Fe(II), (5) Fe(II) oxidation by  $\text{O}_2$ , (6)  $\text{HO}_2/\text{O}_2^{\cdot-}$  photoproduction, (7) bimolecular dismutation of  $\text{HO}_2/\text{O}_2^{\cdot-}$ , (8) Fe(II) oxidation by  $\text{HO}_2/\text{O}_2^{\cdot-}$ , (9) Fe(III) reduction by  $\text{HO}_2/\text{O}_2^{\cdot-}$ , (10) Fe(II) oxidation by  $\text{H}_2\text{O}_2$ , (11) regeneration of  $\text{HO}_2/\text{O}_2^{\cdot-}$  from  $\text{HO}\cdot$ , (12) Fe(III) dark reduction by DOM, (13) dark reduction of surface Fe(III) by DOM, (14) non-reductive dissolution of Fe(III) oxide, (15) sorption of dissolved Fe(II), (16) Fe(III) adsorption/precipitation (Voelker et al. 1997).

Fenton-like reactions play an important role in the scheme of iron reactions. In the Fenton process Fe(II) reacts with  $\text{H}_2\text{O}_2$ , resulting in the formation of Fe(III),  $\text{OH}^-$  and  $\text{OH}\cdot$ , according to equation 1:

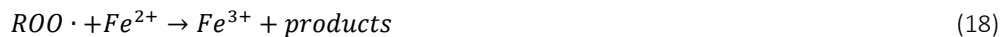


The Fe(III) is reduced again by the  $\text{H}_2\text{O}_2$  resulting in the formation of a peroxide radical and  $\text{H}^+$  (eq. 2):



Thus iron acts as a catalyst for the formation of two very reactive radicals: hydroxyl and peroxide. This process is applied at full scale for the treatment of anoxic groundwater. Further reactions that take place during this process are shown in equations 3 - 18 (Jung et al. 2013):





$Fe^{2+}$  and iron hydroxides are involved in various radical reactions (eq. 4 and 5), e.g. with organic micropollutants or other organic compounds ("R"). When Fenton reactions are applied, it is important to apply an optimal  $Fe^{2+}$  dosage, as the iron can act as a radical scavenger, and may hinder the flow if too high concentrations of dispersed particles are formed. Also the  $H_2O_2$  dosage shows an optimum, both for efficiency of the reaction ( $H_2O_2$  can also act as a radical scavenger), and for the total costs of the process.

pH too is an important factor in the application of Fenton processes for groundwater remediation. In general the optimum pH is considered to be about 3. At  $pH < 3$  the reaction rate of  $H_2O_2$  is decreased by hindrance of the presence of  $(Fe(II)(H_2O))^{2+}$ , and more radical scavenging occurs.  $pH > 4$  the number of free iron ions decreases, and the formation of Fe(II) complexes prevents the formation of free radicals. Besides, Fe(OH)O is formed, reducing the formation rate of  $Fe^{2+}$ .

### Photo-Fenton reactions in sunlit natural water

The effectiveness of Fenton processes may be enhanced by applying UV radiation, using a wavelength of 290-400 nm, resulting in a "photo-Fenton process" (Méndez-Arriaga et al. 2010):



This process works under certain conditions also at neutral pH conditions. Natural organic matter (NOM) is a well-known species that enhance the photo-Fenton process under neutral pH conditions. According to Southworth and Voelker (2003) and Zepp et al. (1992) the photo-Fenton reaction can occur in sunlit natural waters and thus contribute to the oxidation of organic substances, like micropollutants, and the transformation of natural organic

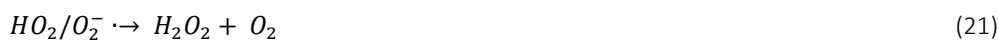
matter into bioavailable compounds. Both reactants of the photo-Fenton reactions (Eq. 1):  $\text{H}_2\text{O}_2$  and  $\text{Fe(II)}$ , are photochemically produced in sunlit natural waters, in the presence of oxygen. The concentrations of both  $\text{Fe(II)}$  and  $\text{H}_2\text{O}_2$  determine the rate of the  $\text{OH}\cdot$  production in sunlit fresh water according to:

$$\frac{d[\text{OH}\cdot]}{dt} = k_{\text{Fenton}} [\text{Fe(II)}][\text{H}_2\text{O}_2]$$

Where [i] refers to the concentration of species i and  $k_{\text{Fenton}}$  ( $\text{M}^{-1}\text{s}^{-1}$ ) denotes the rate constant of the reaction between  $\text{Fe(II)}$  and  $\text{H}_2\text{O}_2$ . The  $\text{Fe(II)}$  availability is critical in the yield of the  $\text{OH}\cdot$  production. A crucial question is whether enough  $\text{Fe(II)}$  is present in sunlit waters to turn over a significant fraction of the photo produced  $\text{H}_2\text{O}_2$ . Iron(II) concentrations are high enough in systems at acidic pH where the oxidation of  $\text{Fe(II)}$  by oxygen is slow but it is still not clear if this is the case for circumneutral pH systems. Vermilyea and Voelker (2009) showed results where enough  $\text{Fe(II)}$  was produced in situ at two field sites at circumneutral pH to compete with biological sinks of  $\text{H}_2\text{O}_2$  and promote the Fenton reaction. They calculated a  $\text{OH}\cdot$  production rate of from the photo-Fenton reaction of  $64 \pm 31 \text{ nM OH}\cdot/\text{h}$  in natural sunlit waters at circumneutral pH.

### Hydrogen peroxide production in sunlit natural water

Hydrogen peroxide is produced in natural waters from the disproportionation of superoxide ( $\text{HO}_2/\text{O}_2\cdot^-$ ), which is formed from the reduction of  $\text{O}_2$  by photo-excited dissolved organic matter (R) (Eq. 20 and 21; reaction 6 and 7 in Figure 2.1) (Cooper and Zika 1983). The apparent yields of  $\text{H}_2\text{O}_2$  production have been determined in a number of studies and do not seem strongly dependent on the sources of the DOM (Andrews et al. 2000, Cooper and Zika 1983). Hence,  $\text{H}_2\text{O}_2$  it is ubiquitous present in natural waters with typically range from less than 10 nM overnight to 400 nM at midday (Cooper et al. 1988, Herrmann et al. 2015) with some lakes reaching as high as 1000 nM (Häkkinen et al. 2004).



Mostafa and Rosario-Ortiz (2013) calculated that the surface steady state concentrations of singlet oxygen ( $^1\text{O}_2$ ), which is a very reactive component, ranges from 1.23 to  $1.43 \cdot 10^{-13} \text{ M}$  for bulk wastewaters under simulated sunlight.

### Iron(II) production in sunlit natural water

Iron(II) is produced in natural waters by photo-reduction of dissolved  $\text{Fe(III)}$  by DOM (reaction 1 in Figure 2.1) or photo-reductive dissolution of  $\text{Fe}$ -hydroxides (reaction 2 in Figure 2.1). The photochemically formed superoxide radical  $\text{O}_2\cdot^-$  plays a role in this process, although colloidal  $\text{Fe(III)}$  and some  $\text{Fe(III)}$  complexes don't react with the radical (Henneberry et al. 2012, Voelker and Sedlak 1995). Southworth & Voelker (2003) have calculated that if enough  $\text{Fe(II)}$  is present to outcompete other decreases in  $\text{H}_2\text{O}_2$  concentration, the Fenton reaction could be by far the dominant source of  $\text{OH}\cdot$  in sunlit natural waters leading to a significant removal of organic compounds in sunlit natural waters.

Photoreduction of  $\text{Fe(III)}$  is rapid in acidic solution but the reaction rate decreases sharply as the pH increases. However, complexation of iron by carboxylate ligands such as oxalate, citrate and DOM increases photoreduction rates by increasing the  $\text{Fe(III)}$  solubility, the absorption of visible light by  $\text{Fe}$  complexes, and the yield of  $\text{Fe(II)}$  per photon absorbed by the  $\text{Fe(III)}$  complex (Southworth & Voelker, 2003). Nanomolar concentrations of  $\text{Fe(II)}$  have been measured in both seawater and alkaline freshwater, although the rapidity of  $\text{Fe(II)}$  oxidation at circum-neutral and alkaline pH values makes it difficult to obtain accurate measurements.

According to Kim et al. (2019) dissolved organic matter (DOM) can extract Fe(III) from soil by complexation. The complexes formed can react under the influence of sunlight, forming Fe(II). Kügler et al. (2019) point out that the stability of Fe(III) and Fe(II)-DOM complexes may vary. The more labile complexes dominate the upper, oxic layer (0-10 cm) in fens, whereas more stable complexes are found in lower, anoxic layer (15-30 cm). Fe(III) complexation with humic acids depends on pH (Catrouillet et al. 2014).

Xing et al. (2019) describe two major pathways for the photochemical reduction of Fe(III) in sunlit surface waters. One is the ligand-to-metal charge transfer (LMCT) and the other the superoxide mediated iron reduction (SMIR) process. Photolabile Fe(III)-NOM complexes are rapidly reduced by LMCT, while  $O_2^{\bullet-}$  is not involved in these reduction processes. However, the relatively less photolabile amorphous ferrous oxide (AFO) can be reduced by both pathways. The reduction of AFO by  $O_2^{\bullet-}$  occurs following the dissolution of AFO, and thus the contribution of  $O_2^{\bullet-}$  depends on conditions like the AFO age and initial concentration, which affect the rate of dissolution. The  $O_2^{\bullet-}$  mediated iron reduction is only important in natural waters containing limited concentrations of Fe binding ligands. This is summarized in Figure 3.

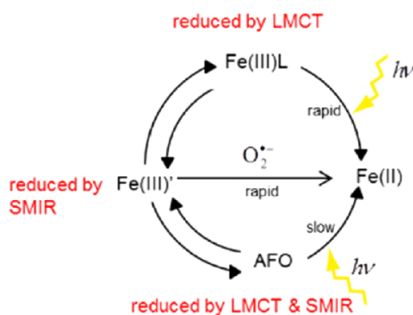


Figure 3: schematic overview of Fe reduction and oxidation processes (Xing et al. 2019)

The SMIR route is more likely to occur in coastal waters rather than in open oceans, since over 99% of the total iron present is expected to be in organically complexed form in open oceans. However, the concentration of suspended iron oxyhydroxides is expected to be higher in iron-rich coastal environments.

Solar radiation results in the formation of short-lived organic compounds, relatively stable semiquinone-like compounds and hydroperoxy radicals (Garg et al. 2013a, Garg et al. 2013b). The reactions taking place under light conditions are schematically shown in Figure 4.

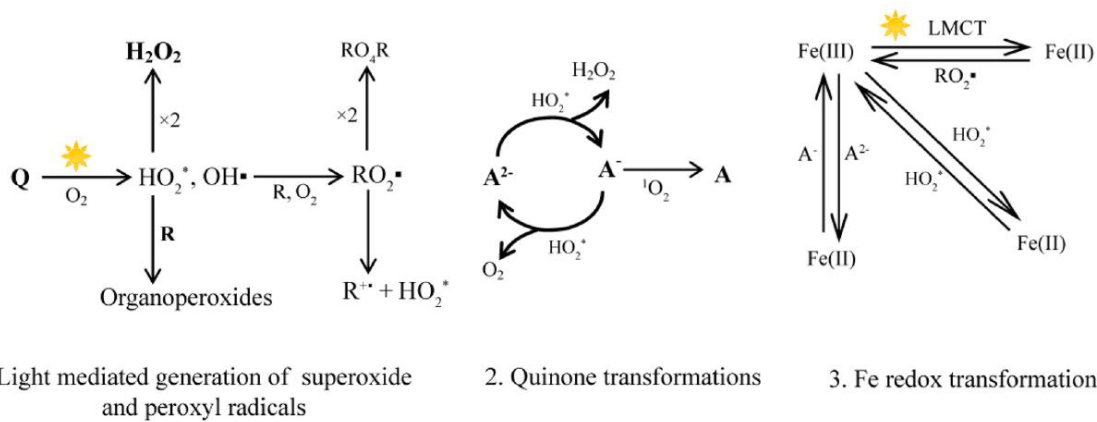


Figure 4: Reaction scheme of the redox transformation of Fe and electron formation of Fe(III) reductants and Fe(II) oxidants during irradiation of NOM at pH 4 (Garg et al. 2013a, Garg et al. 2013b)

Highest concentrations of Fe(II) in the steady state were observed at pH > 5.5. In the absence of organic complexes 30-70% of the dissolved iron in areas with sun light occurs as Fe(II) during daytime. In the dark the Fe(II) is quickly oxidized to Fe(III). The different processes taking place in light and under dark conditions are shown in Figure 5.

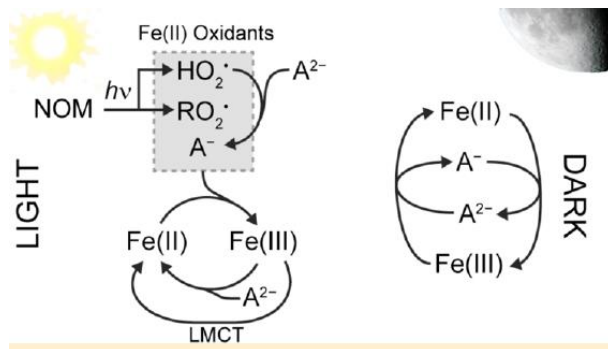


Figure 5: Oxidation and reduction of Fe under light and dark conditions (Garg et al. 2013b)

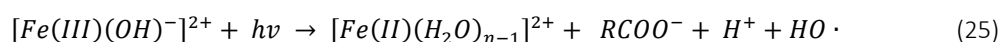
According to Garg et al. (2015) Fe species undergo continual cycling between Fe(II) and Fe(III) oxidation states. The transformations are far more dynamic in sun light than in the dark, as shown in Table 1.

Table 1: turnover frequency of Fe(II) – Fe(III) ( $h^{-1}$ ) as a function of pH in the presence of 10 mg of SFRA (Suwannee River Fulvic Acid) (Garg et al. 2015).

pH	light	dark
3	17.3	1.9
3.5	27.4	2.5
4	33.2	2.9

Meunier et al. (2005) studied the effects of size and origin of natural dissolved organic matter compounds (DOM) on the redox cycling of iron in different environmental setting ranging from freshwater systems to marine systems. Their results show that Fe(II) steady-state concentrations in irradiated seawater samples, both as percentage of total dissolved iron and normalized to 1 mg C L<sup>-1</sup>, were higher in the low-molecular-weight (LMW) than in the high-molecular-weight (HMW) DOM fractions, despite higher net rates of H<sub>2</sub>O<sub>2</sub> formation in the HMW DOM fractions. However, although in fresh water (Lake Murten) similar results were obtained for the Fe(II) concentration, here the H<sub>2</sub>O<sub>2</sub> formation rate appeared to be higher for the LMW DOM fraction. Their results also suggested that that DOM derived from terrestrially sources has a higher photochemical reactivity towards Fe(II) formation than autochthonous DOM which is formed in the surface water body.

Organic matter (especially carboxylates) plays a crucial role in this redox cycling between pH 3.0 and 6.7 (Karlsson and Persson 2012). According to Nichela et al. (2015) factors that affect the reduction of Fe(III) species are the formation of Fe(III)-HBA complexes (hydroxyl derivatives of benzoic acid), the ability of these complexes to participate in reductive pathways, and the formation of intermediate products capable of reducing ferric species. The presence of stable bidentate ferric complexes in acidic aqueous solutions (pH ≈ 3) decreases the overall degradation rates in Fenton systems by slowing down the Fe(II) formation through both dark and photo-initiated pathways. Under dark conditions at acidic pH, hydroquinone groups intrinsically present in the NOM induce reduction of Fe(III) to Fe(II). Thus semiquinone groups are formed, which in turn can re-oxidize Fe(II) to Fe(III). Photolysis of the NOM results in the formation of superoxides, which in turn induce the oxidation of hydroquinone to semiquinone moieties. Their concentrations increase with increasing pH. Under dark conditions these moieties are relatively stable. Irradiation of NOM results in the generation of both long-lived and short-lived Fe(II) oxidants. Dioxygen plays an important role in the production of the long-lived Fe(II) oxidant, as the formation of super-oxide occurs via the reduction of dioxygen. The processes that occur under dark conditions differ from those that occur under light conditions. Ligand to metal charge transfer (LMCT) processes dominate Fe(III) reduction at low pH values (Garg et al. 2015). Ferric complexes of aliphatic carboxylates undergo a photo-induced decarboxylation upon excitation by wavelengths in the 300-400 nm range, whereas ferric-salicylate complexes yield Fe(II) and hydroxyl radicals by oxidation of water molecules in the coordination sphere of the metal center. Their efficiencies, however, are significantly lower than those of the Fe(III) aqua complex. Fe(III)-HBA complexes cannot be photolyzed in this wavelength range. In accordance with the publications of Garg et al., Nichela et al. (2015) found that hydroquinone-like structures are very efficient for the reduction of Fe(III), whereas catechol-like structure were much less efficient. Radicals can be produced from the oxidation of either the organic ligand (reaction 22) of a water molecule in the coordination sphere (reactions 23 and 24). Another pathway is the electrophilic attack of hydroxyl radicals formed according to reaction 25



For aliphatic acids like oxalate, pyruvate, tartrate and citrate photolysis of ferric complexes takes place through ligand decarboxylation (reactions 23 and 24). Complexation of Fe(III) slows down the formation of Fe(II) under dark conditions, both for aliphatic and aromatic carboxylates. The enhancement of the Fenton process upon irradiation is smaller for aromatic carboxylates than for ferric aliphatic carboxylates. Reaction 25 results in the formation of stoichiometric amounts of Fe(II) and hydroxyl radicals, but with substantially lower efficiencies than that of the

Fe(III)aqua complex. The efficiency of the Fe(III) reduction largely depends on the structure and amounts of reducing intermediates. Hydroquinone-like structure are far more efficient than catechol-like structure, whereas dihydroxybenzene derivatives with a resorcinol-like structure were unable to reduce Fe(III) to Fe(II) (see Figure 6 ). Trihydroxy benzoic acid derivatives efficiently produce Fe(II), but ring opening reactions and decomposition prevail under Fenton conditions.

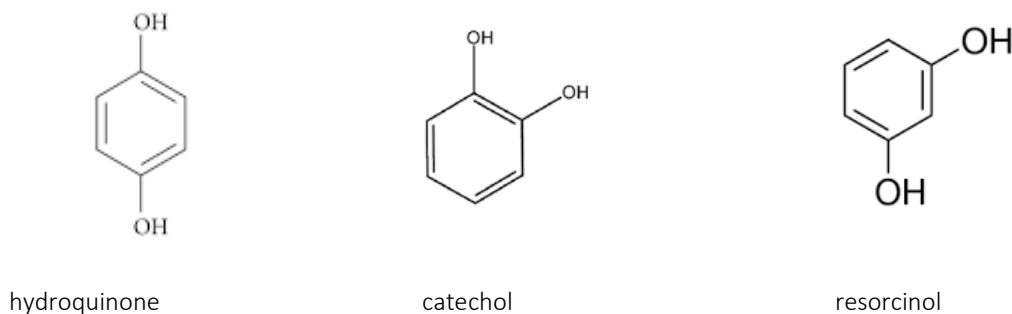


Figure 6: chemical structure of hydroquinone, catechol and resorcinol. Hydroquinones are the most effective, resorcinol-like compounds are the least effective in Fe(III) reduction.

This is in accordance with the findings of Du et al. (2020), who found that ROS generation is related to the NOM dissociation constant, which explains the effect of pH and different NOM structures. Marchisio et al. (2015) give an overview of the quantum yields for the formation of chromophoric dissolved organic matter (CDOM) triplet states ( $^3\text{CDOM}^*$ ), singlet oxygen ( $^1\text{O}_2$ ) and hydroxyl radicals ( $\text{HO}\cdot$ ). The quantum yields depend on the wavelength, in the order UVB > UVA > blue.

Lee et al. (2017) investigated the oxidation and reduction kinetics of iron and the steady-state ratio of Fe(II) concentration: total dissolved Fe in the presence of various types of humic substances. The reaction rates could vary by up to a factor 10 for photochemical reduction and a factor 7 for thermal reduction. For the Fe(II) oxidation variations in reaction rate up to a factor 15 were observed in  $\text{H}_2\text{O}_2$  mediated reactions, and up to a factor 3 for  $\text{O}_2$  mediated reactions. The variation of the Fe(II) oxidation appeared to be associated with the aliphatic content of the NOM, suggesting that Fe(II) complexation by aliphatic compounds accelerates Fe(II) oxidation. Although the Fe(III) coordination by carboxyl groups is important in LMCT processes, no strong relations were observed between the photochemical reduction of Fe(III) and the carboxyl content of the NOM. Also pH plays an important role. The steady-state Fe(II) fraction appeared to be higher at pH 7.0 than at pH 8.0 under light conditions. Compared to dark conditions, the steady-state Fe(II) fraction in the presence of (simulated) sunlight increased by 20-fold at pH 7 and by 16-fold by pH 8. The differences observed for both pH values can be explained from faster photochemical and thermal reduction and slower oxidation rates for pH 8. The authors also found that anthropogenic inputs from e.g. sewage effluents and agricultural drainage may affect the Fe redox kinetics in natural waters.

Garg et al. (2015) studied the effect of sunlight, and concluded that Fe(II) generation rates resulting from Fe(III) reduction were substantially lower in previously irradiated NOM solutions than those observed under dark conditions. However, the reduction rates of Fe(III) during photolysis could be either higher or lower depending on the importance of LMCT at acidic pH. In natural sunlit environments where humic or fulvic-type NOM is present under mildly acidic conditions, steady state Fe(II) concentrations are much lower than would be the case if Fe(II) oxidation was controlled by the presence of either  $\text{O}_2$  or  $\text{H}_2\text{O}_2$  only. Fe(II) oxidant formed by the photolysis of NOM

may be long-lived, as a result of which Fe(II) concentrations decrease once sunlight mediated Fe(II) generation ceases in a sunlit water body. The influence of pH was described in a subsequent paper (Garg et al. 2018). On solar irradiation a part of the hydroquinone-like compounds present are transformed into semiquinones, that are capable of reducing Fe(III) or oxidizing Fe(II) under circum-neutral pH conditions. The extent of photo generation of semiquinones by irradiation of NOM and the persistence of these radicals increases significantly with decreasing pH values. Due to the higher concentrations and longevity of these semiquinones under acidic conditions, the impact of pH on steady-state Fe(II) concentration is less pronounced in previously irradiated NOM solutions than in dark solutions. Under irradiated conditions the rates of Fe transformation (including both Fe(II) oxidation and Fe(III) reductions) are almost independent of pH. While LMCT was found to be the dominant pathway for photochemical Fe(III) reduction, Fe(II) oxidation under irradiated conditions mainly occurs as a result of interaction with O<sub>2</sub>, semiquinones and other short-lived oxidants. As a result the steady-state Fe(II) concentration in irradiated surface waters containing NOM doesn't significantly depend on pH changes.

Overviews of kinetic parameters found in literature are given in Table 3 to Table 8 in Appendix I.

### 2.2.2 Biologically induced redox cycling of iron

In the previous paragraph attention was paid to the redox cycling of organic iron complexes. However, it is also possible that micro-organisms are involved in the redox cycling of iron. Gault et al. (2011) discuss bacteriogenic iron oxides (BIOS) in neutral groundwater, which can either cause oxidation or reduction of iron. Fritzsche et al. (2012) describe the microbial reduction of iron complexes in anoxic soil. Wang et al. (2017) studied the photochemical properties of the organic exudate secreted by a toxic strain of *Microcystis Aeruginosa* (see Figure 7), by measuring reactive oxygen species (ROS) generation and redox transformations of iron in the presence of this exudate at pH 4 and 8. The organic exudate generates nanomolar concentrations of superoxide and H<sub>2</sub>O<sub>2</sub> during irradiation with (simulated) sunlight. Under alkaline conditions this superoxide is responsible for the production of nearly 45% of the observed Fe(II) from Fe(III) reduction. The rest of the Fe(III) reduction occurs via the LMCT pathway. Under acidic conditions 100% of the Fe(III) reduction occurs via the LMCT pathway. It was suggested that steady-state dissolved Fe concentrations in natural water will significantly increase in the presence of algal exudates. Furthermore, they state that a significant diel variation in Fe(II) concentration can be expected, even in acidic waters, as the time scales of light-mediated Fe(III) reduction and thermal Fe(III) reduction differ markedly. In the dark no iron reduction was observed at pH 4 and 8.

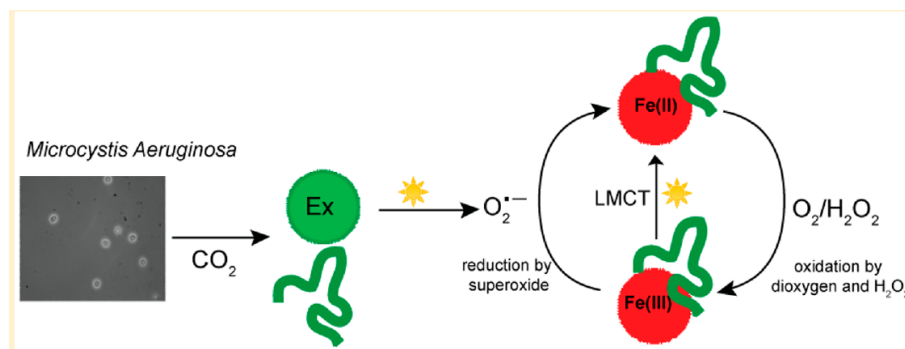


Figure 7: Light mediated ROS generation and Fe redox transformations in the presence of exudate from the Cyanobacterium *Microcystis Aeruginosa* (Wang et al. 2017)

Samperio-Ramos et al. (2018) describe the role played by natural organic ligands excreted by the cyanobacteria *Synechococcus* PCC 7002 on the iron redox chemistry, at pH 7.2 – 8.2, temperature 5 – 35 °C, and different salinity-values. The observed a pH dependent and photo-induced Fe(III) reduction process in the presence of exudates

produced under Fe-low conditions. Photolytic reactions also modified the reactivity of those exudates with respect to Fe(II), increasing its lifetime in seawater. Under dark conditions the organic ligands excreted under Fe deficient conditions enhanced the Fe(II) oxidation at pH < 7.5. The organic exudates released at high iron concentrations retarded the Fe(II) oxidation, as a function of DOC produced.

According to Kulkarni et al. (2018) humics-enhanced microbial reductive dissolution by iron reducing bacteria (IRB) occurs, in which dissolved humic acids (DOM) may serve as electron shuttles to accelerate Fe(II) release and mobilization. Micro-organisms use humic substances, including fulvic acid, as electron shuttles during Fe(III) reduction in anaerobic soils and sediments. This is schematically shown in Figure 8.

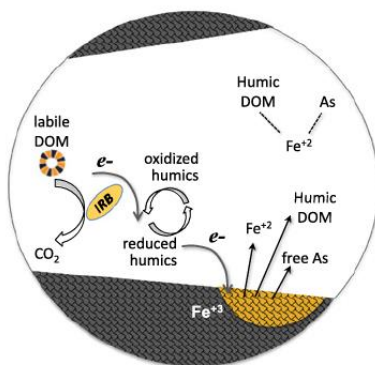


Figure 8: microbial iron reduction (Kulkarni et al. 2018)

DOM complexes with iron greatly influence the microbial iron redox cycling, by serving as electron shuttles (Kügler et al. 2019). Wordofa et al. (2019) studied the fate and stability of organic compounds during microbial reduction of Fe(III). They used glucose (GL), glucosamine (GN), tyrosine (TN), benzoquinone (BQ), amylose (AM), and alginate (AL), complexed with an Fe oxide mineral, ferrihydrite (Fh). During 25 days of anaerobic incubation with *Shewanella putrefaciens* CN32, the reduction of Fe followed the order of Fh-BQ > Fh-GL > Fh-GN > Fh-TN > Fh-AL > Fh-AM. Organic carbon regulated the reduction of Fe by acting as an electron shuttle, affecting microbial activities and associating with Fh. Benzoquinone had the highest electron accepting capacity, but potentially can inhibit microbial activity. Liu et al. (2020) applied the redox cycling of manganese and iron for the anaerobic biodegradation of micropollutants like metoprolol. Fe(III) here is used as the electron acceptor.

An overview of kinetic data for this topic is shown in Table 9 in Appendix I.

### 2.2.3 Degradation of organic micropollutants by (indirect) photolysis of surface waters

As was already briefly mentioned in the previous sections, during iron redox cycling active compounds like hydroxyl radicals, hydrogen peroxide, superoxide anions, singlet oxygen and organic radicals may be formed. These compounds may react with organic micropollutants, thus improving the water quality. Vermilyea and Voelker (2009) state that in this way biologically or chemically recalcitrant organic compounds in surface water at circum-neutral pH may be degraded. This was also mentioned by (Liu et al. 2020), Southworth and Voelker (2003) and Mostafa and Rosario-Ortiz (2013).

Bodhipaksha et al. (2017) studied the degradation of four common compounds in wastewater. They found that sulfamethoxazole is primarily degraded via direct photolysis with some contribution from hydroxyl radicals and

possibly carbonate radicals or other unidentified organic radicals. Sulfadimethoxine also is degraded mainly by direct photolysis, and NOM appeared to inhibit this process. However, in the presence of organic matter, sulfadimethoxine appeared to react with hydroxyl radicals and singlet oxygen. Another pollutant, Cimetidine, was mainly degraded by reaction with  $^1\text{O}_2$ , whereas caffeine was found to mainly react with  $\text{HO}\cdot$ . Calisto et al. (2011) describe the direct and indirect photodegradation of psychiatric pharmaceuticals (oxazepam, diazepam, lorazepam and alprazolam) under simulated solar irradiation. It was observed that humic acids hinder the degradation of these compounds, whereas fulvic acid caused an enhancement of the photodegradation. Sur et al. (2012) show that 2-nitro-4-chlorophenol (NCP; a nitroderivative of 4-chlorophenol, which is a transformation intermediate of the herbicide dichlorprop) was effectively degraded by direct photolysis and by reaction with hydroxyl radicals, formed in surface water. Marchetti et al. (2013) describe the degradation of atrazine in surface water by photolysis, reaction with hydroxyl radicals, and with triplet states of chromophoric dissolved organic matter  $^3\text{CDOM}^*$ . These  $^3\text{CDOM}^*$  also play a role in the degradation of pollutants like phenols, phenylurea herbicides and sulfonamide antibiotics (Vione et al. 2014). For singlet oxygen these authors state that its reactivity is not confined to the bulk aqueous phase, but has a microheterogeneous distribution within DOM and can reach high steady-state concentrations in the hydrophobic sites of DOM, sometimes much higher than in the bulk aqueous solution. In this way it can induce effective degradation of hydrophobic pollutants.

Batista et al. (2016) studied the role of NOM in the removal of sulfamerazine (SMR: a sulfonamide antibiotic) from aquatic environments. They concluded that the chemical composition of NOM plays a very important role. Aldrich humic acid, with a high aromatic and low protein/carbohydrate content appeared to be the most reactive NOM for the degradation of SMR. Aromaticity and the specific UV absorption at 254 nm ( $\text{SUVA}_{254}$ ) were found to be potential indicators of NOM hydroxyl radical reactivity. According to Chen et al. (2017) humic substances play an important role in the degradation of naproxen by simulated sunlight. Both direct and indirect photodegradation of naproxen decreased with increasing pH, which was consistent with the trend of singlet oxygen reaction rate constants of naproxen. Humic acids appeared to significantly hinder the photodegradation. The direct photodegradation of naproxen was ascribed to the decomposition of the excited triplet state of naproxen and self-sensitization effect involving singlet oxygen. Fulvic acids mainly were involved in reactions with singlet oxygen in aerated solutions.

In addition to the factors described in previous paragraphs, the steady-state Fe(II) concentrations depends also on the availability of iron in the surface water system. Dissolved or colloidal Fe(III) complexes with organic matter are more photoreactive than more crystalline iron precipitates. In addition, amorphous iron oxyhydroxide preparations are much more easily photoreduced than ferrihydrite (Vermilyea and Voelker 2009). Hence, surface water reservoirs where drinking water companies apply iron to remove phosphate for the surface water have conditions favorable for enhanced steady-state Fe(II) concentration compared to reservoirs without iron dosing.

Drinking water companies use  $\text{FeCl}_3$  or  $\text{FeSO}_4$  for phosphate removal in their surface water reservoirs. Freshly formed iron oxyhydroxides produced by the application of  $\text{FeCl}_3$  or  $\text{FeSO}_4$ , either in colloidal form or as suspended sediment in the water column likely result in a relative large pool of easily photo reducible Fe(III) and thus in relatively high steady state concentrations of Fe(II) during daytime. In the case of  $\text{FeSO}_4$ , the steady state Fe(II) concentrations are likely high due to the constant dosing of  $\text{FeSO}_4$ . Oxidation of Fe(II) by oxygen results also in production of  $\text{H}_2\text{O}_2$  and thus in enhancing the Fenton reactions. Surface water reservoirs with iron application may thus have a higher potential for degradation of organic micro contaminant than system without iron application.

Although in the above mentioned examples the iron redox cycling isn't mentioned, from the previous paragraphs it can be concluded that the reactive species formed during this redox cycling are identical to the reactive species

mentioned here. Therefore, it is to be expected that also during redox cycling organic micropollutants may be degraded. This effect may be strengthened by dosing Fe to surface water reservoirs.

## 2.3 Reductive pathway

### 2.3.1 Chemical processes

Numerous reports have shown that the combination of dissolved Fe(II) and Fe(III)-bearing minerals are a potent reductant for many reducible organic and inorganic contaminants including nitroaromatics (Elsner et al. 2004, Hartenbach et al. 2006, Klausen et al. 1995, Strehlau 2016), chlorinated solvents (Buchholz et al. 2011, Elsner et al. 2004), pesticides (Sivey and Roberts 2012, Strathmann and Stone 2003), antibiotics (Mohatt et al. 2011). These studies have demonstrated that reaction rates increase dramatically when iron oxide or oxyhydroxide mineral surfaces are present.

The mechanism driving this phenomenon is studied by earlier workers (e.g. Stumm 1987). The reduction of oxidized contaminants by Fe(II) in the presence of an iron oxide mineral surface occurs via three steps (Strehlau 2016) (Figure 9). First, adsorption of Fe(II) occurs by complexation to surface hydroxyl groups on the iron oxide. An overlap in Fe(II) and Fe(III) d-orbitals results in electron delocalization. This means that electrons are not associated with a single atom or a covalent bond but that they are extended over several adjacent atoms. Electron delocalization results in an overall decrease in the redox potential of Fe(II)-Fe(III) couple, therefore stabilizing the Fe(III) oxidation state making the transfer of an electron from Fe(II) more favourable (Farley et al. 1985, Schaefer et al. 2011, Stumm 1987). Specifically for minerals that contain Fe(III) in their bulk structure, like iron oxides, electron delocalization is not always limited to the mineral surface but instead can occur within the bulk mineral. This second stage is described as interfacial electron transfer (Williams and Scherer 2004). Interfacial electron transfer has been demonstrated for various iron oxides in the presence of aqueous Fe(II), including hematite, goethite, and others (Rosso et al. 2003, Williams and Scherer 2004). Finally, during the third stage, the contaminant species nears the surface of the iron oxide and electron transfer occurs, resulting in a chemically reduced contaminant (Strehlau 2016).

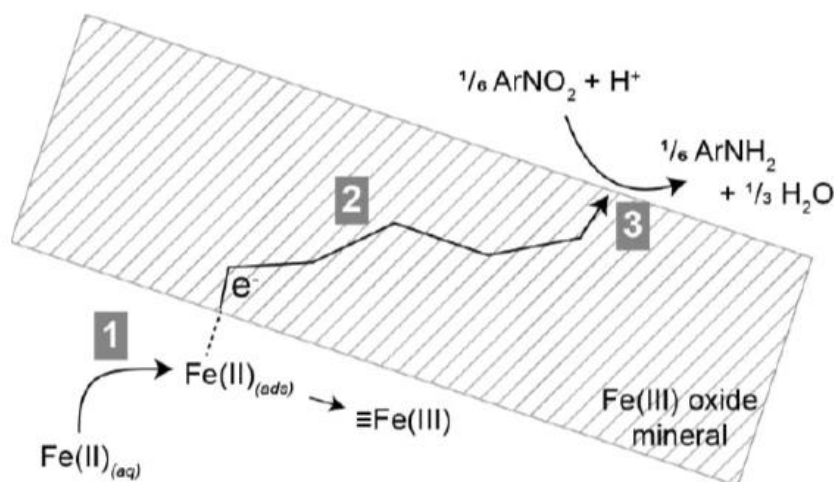


Figure 9. Schematic illustration of the reduction of a nitroaromatic compound by surface-mediated reaction with Fe(II). 1) Adsorption of Fe(II) and electron delocalization at the mineral surface. 2) Interfacial electron transfer within the bulk mineral. 3) Approach of a nitroaromatic compound at the mineral surface and subsequent electron transfer (from Strehlau 2016).

Williams and Scherer (2004) reported observations of Fe(II) reacted with oxide surfaces under conditions typical of natural environments (i.e., wet, anoxic, circumneutral pH, and about 1% Fe(II)) using the isotope specificity of  $^{57}\text{Fe}$  Mössbauer spectroscopy. Mössbauer spectra of Fe(II) adsorbed to rutile ( $\text{TiO}_2$ ) and aluminum oxide ( $\text{Al}_2\text{O}_3$ ) show only Fe(II) species, whereas spectra of Fe(II) reacted with Fe(III) oxides: goethite, hematite, and ferrihydrite, demonstrate electron transfer between the adsorbed Fe(II) and the underlying Fe(III) oxide. Electron-transfer induces growth of an Fe(III) layer on the oxide surface that is similar to the bulk oxide. The resulting oxide is capable of reducing nitrobenzene, but interestingly, the oxide was only reactive when aqueous Fe(II) is present (Figure 10).

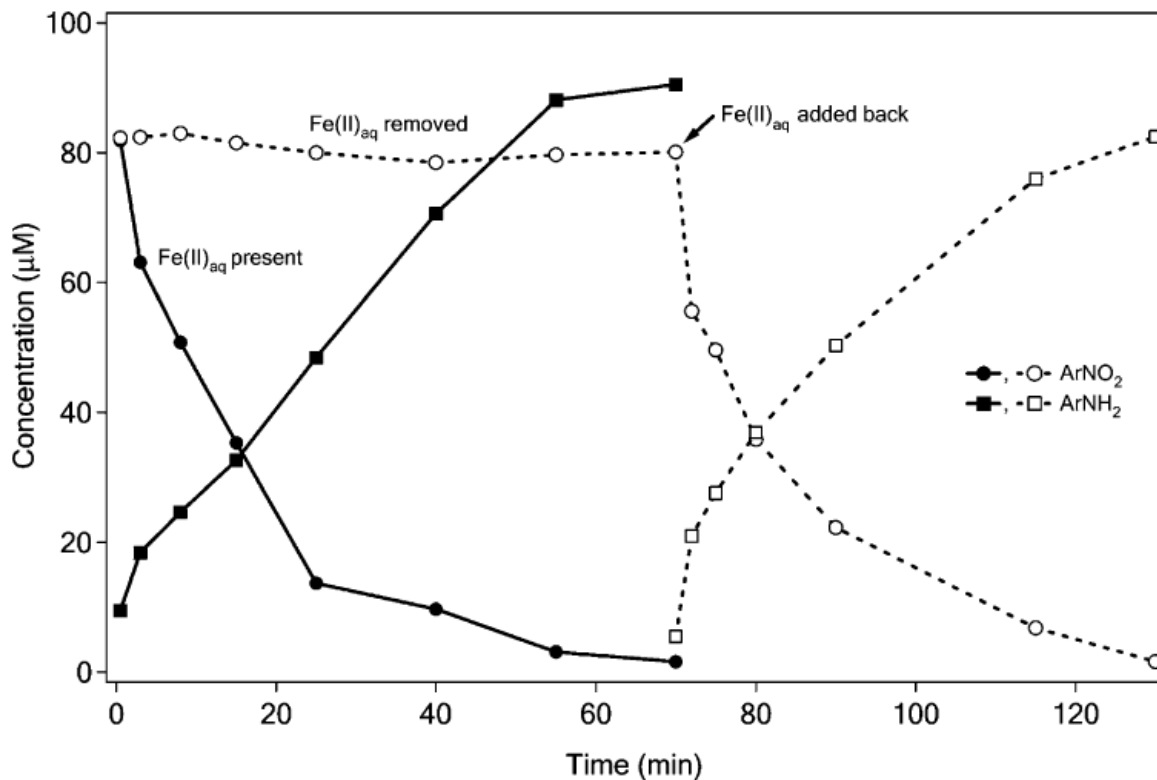


Figure 10. Reduction of nitrobenzene by Fe(II) "adsorbed" on goethite in the absence and presence of aqueous Fe(II). Experimental conditions: 30 mg of the goethite, pH 7.4, and an initial aqueous Fe(II) concentration of 1 mM (achieved by adding  $\text{FeCl}_2$ ). Control experiments confirmed that no  $\text{ArNO}_2$  was removed from solution in the presence of goethite or aqueous Fe(II) alone (from Williams and Scherer 2004).

Elsner et al. (2004) reported surface-area-normalized pseudo first-order rate constants for the degradation of the reducible organic compounds hexachloroethane, 4-chloronitrobenzene (and the intermediate 4-chlorophenyl hydroxylamine) in a system containing a Fe(II) solution with different iron minerals in suspension (Figure 11). These compounds represent two classes of environmentally relevant transformation reactions of pollutants, i.e., dehalogenation and nitroaryl reduction. The results of Elsner et al. (2004) showed that the reactivities of the different Fe(II) mineral systems varied greatly and systematically both within and between the data sets obtained with the two compounds. As a general trend, surface-area-normalized reaction rates increased in the order Fe(II) +

siderite < Fe(II) + iron oxides < Fe(II) + iron sulfides. 4-Chloronitrobenzene was transformed by mineral-bound Fe(II) much more rapidly than hexachloroethane, except for suspensions of hematite and pyrite.

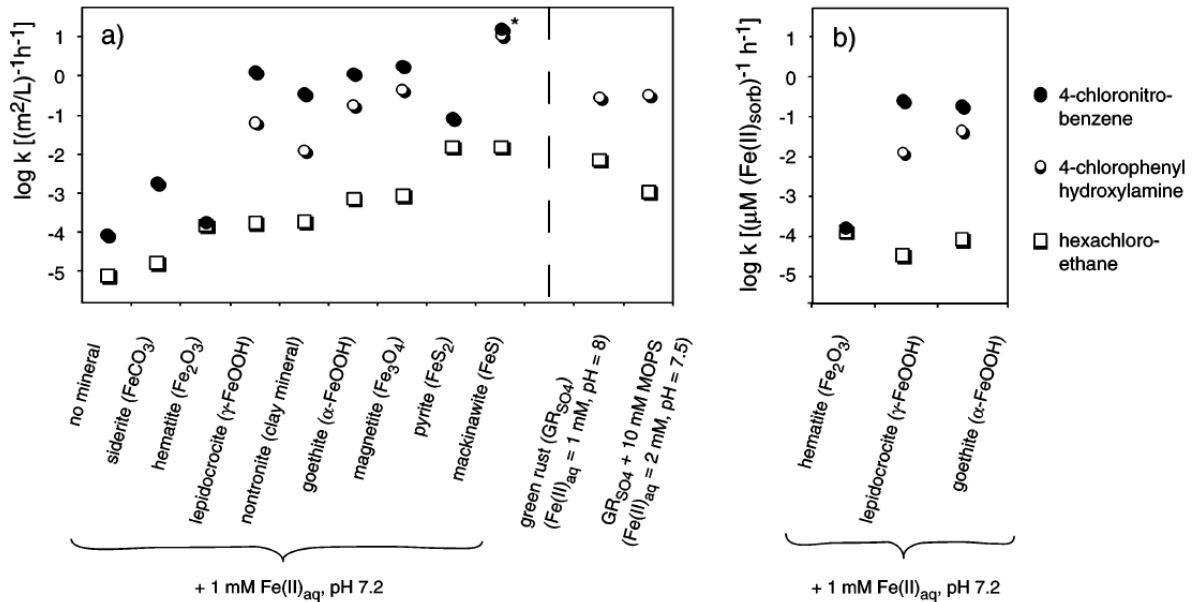


Figure 11 Logarithmic pseudo-first-order rate constants for the reaction of different Fe(II) containing minerals with the reducible organic compounds hexachloroethane, 4-chloronitrobenzene, and the intermediate 4-chlorophenyl hydroxylamine. (a) Surface area-normalized, (b) normalized to sorbed Fe(II). The asterisk (\*) indicates likely mass transfer limitation (from Elsner et al. 2004).

The study of Strathmann and Stone (2003) examined the reduction of oxime carbamate pesticides (oxamyl, methomyl, and aldicarb) by Fe(II) in aqueous suspensions containing twelve different (hydr)oxide and aluminosilicate minerals. In the absence of Fe(II), mineral surfaces have no apparent effect on the pathways or rates of oxime carbamate degradation. In anoxic suspensions containing Fe(II) and mineral surfaces, rates of oxime carbamate reduction are significantly faster than in equivalent mineral-free homogeneous solutions. Reduction rates increase with increasing surface area loading (mineral surface area per volume of suspension) and pH (Figure 12). The results indicate a first-order dependence on total adsorbed Fe(II) concentration and no significant dependence on adsorbed oxime carbamate concentration.

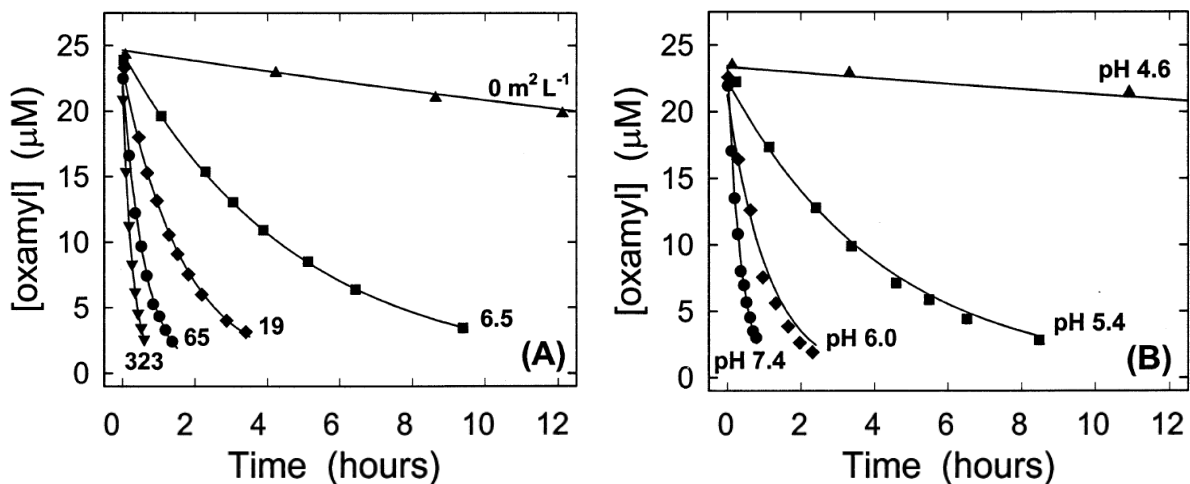


Figure 12. Oxamyl reduction by 0.5 mmol/L Fe(II) in the presence of hematite: (A) Effect of varying surface area loading ( $S_{AL}$ ,  $m^2/L$ ) at pH 7.4; (B) effect of varying pH in the presence of 129  $m^2/L$  hematite. Symbols indicate measured concentrations and lines indicate pseudo first-order model fits. Reaction conditions: 0.5 mmol/L total Fe(II), 25 mol/L oxamyl, 25°C, 100 mmol/L NaCl, pH 4.6 to 7.4,  $S_{AL}$  0 to 323  $m^2/L$  (from: Strathmann and Stone 2003)

### 2.3.2 Potential effect of subsurface iron removal

Subsurface iron removal (SIR) is an in-situ technique to lower the Fe content of extracted groundwater. Through cyclic injection of oxygenated water Fe(II) oxidises and precipitates as Fe hydroxide in a zone surrounding the extraction well, enhancing the sorptive capacity of the aquifer (Vandenbohede et al. 2019). During subsequent pumping phases, suboxic or anoxic groundwater traverses the oxidation zone and Fe(II) iron sorbs to available and newly formed exchange and sorption sites, thereby retarding the breakthrough of dissolved iron.

This cycling of injection of oxygenated water followed by abstraction of anoxic and suboxic Fe(II)-bearing groundwater results in the ubiquitous presence of Fe hydroxides on which Fe(II) ions sorb. This environment is favourable for the degradation of reducible organic contaminants. Groundwater contaminants that undergo reductive dehalogenation may thus degrade in the environment nearby a groundwater well where SIR is applied. Typical examples of these compounds are chlorinated solvents like perchloroethene (PCE) and trichloroethylene (tri). In addition, a large group of pesticides and pharmaceuticals degrades more easily under (deep) anoxic conditions than under oxic conditions, i.e., they are vulnerable for reductive degradation. Typical examples of these compounds are: bentazone, atrazine, lindane and sulfamethoxazole.

Based on our findings in the literature it is very likely that subsurface iron removal may have a positive effect on the near well degradation of organic groundwater contaminant.

## 3 OMP degradation potential

We tried to estimate the OMP degradation potential of Fe redox cycling in sunlit surface waters via the oxidative pathway, and also for anoxic water via the reductive pathway.

### 3.1 The oxidative pathway

The concentration of active compounds that can react with OMPs is assumed to be in the order of magnitude of 1 ng/L. The concentrations of OMPs are in the order of magnitude of  $\mu\text{g/L}$ . Let's assume that 1 ng of active compounds can react with 1 ng of OMP. In fact the comparison should be made on a molar base, but with a molar mass of 56 for iron and 300-700 for OMPs, and the fact that the efficiency of the reaction (the number of Fe-atoms and radicals that successfully react with OMPs) will be lower than 100%, the assumption that 1 ng of Fe-compounds will react with 1 ng of OMP will compensate for the lower efficiency.

The turnover frequency of Fe is about  $30 \text{ h}^{-1}$ , which means that about 30 ng of active compounds will be formed during one hour, or about  $8 \cdot 30 = 240 \text{ ng per day}$ . So this would be enough to degrade about 240 ng of OMP per day.

Let's assume there is  $1 \mu\text{g/L}$  of OMP present, and 90% has to be removed, which is  $0.9 \mu\text{g/L}$ . This would, in this example, take about 4 days.

The depth of e.g. the Biesbosch reservoir is on average 14 m, and sunlight would penetrate only the first 10 cm (the exact penetration depth will depend on the water quality, e.g. the NOM composition). As a result, only  $1/140$  of the basin will be involved in reactions, or in other words, the effective concentration would be  $140 \mu\text{g/L}$ , and it would take  $0.9 \cdot 140 / (240 \cdot 10^{-3}) = 525$  days to degrade the OMP for 90%.

Assume the residence time is 5 months or 150 days, then  $150 \cdot 240 = 3.6 \cdot 10^4 \text{ ng}$  of OMP would be degraded per L. This accounts for 26% degradation of the compounds.

From literature and Dutch investigations it is known that the degree of degradation of OMPs can vary significantly for different reservoirs. For example the degradation rate of OMPs in the reservoir of PWN is very low, whereas in the Biesbosch reservoirs of Evides high degradation rates can be observed. Here the following OMPs were found to be degraded by  $\geq 90\%$ : AMPA, bisoprolol, guanyleurea, ibersartan, metoprolol, sotalol, bisphenol-a, glyphosate, MTBE, gabapentin, DIPE (di-iso propyl ether), hydrochloro thiazide, cyclamate, diclofenac, urotropin, iprodion and levetiracetam.

In Table 2 an overview is given of the reservoirs in the Netherlands and in Belgium (of De Watergroep), their depths and residence times. Applying the calculation shown above, the possible degradation rate of OMPs was estimated. It can be concluded that in some cases significant degradation may be possible, especially if iron could be added (which is not always done).

*Table 2: Overview of reservoirs in the Netherlands and Flanders (De Watergroep), some characteristics, and an estimation of the possible OMP degradation effect. For this estimation, it was assumed that about 240 ng/day would be degraded via the oxidative pathway, and that degradation can only take place in the upper 10 cm of the reservoir. The reservoir is assumed to be fully mixed, so the apparent concentration that has to be degraded in the upper layer is depth/0.10 times as high as the actual concentration in the water. Example: at WML the average*

depth is 20 m, so the concentration that is present equals  $20/0.1 = 200 \mu\text{g/L}$ . during  $1.75 \cdot 365 = 639$  days. During this period  $639 \cdot 240 \cdot 10^{-3} = 153 \mu\text{g/L}$  can be degraded, which is about  $153/200 \cdot 100\% = 77\%$  reduction.

Reservoir	depth	residence time	Fe dosage	Theoretically possible OMP degradation effect (%)
De Punt, WBG	≤ 19 m	48 – 58 days	insufficient effective for phosphate removal	7
Lange Vlieter, WML	≤ 35 m, on average 20 m	1.5-2 years	yes	77
Waterleidingplas Waternet	≤ 17m, 5 m on average	3 months	yes	43
Blankaart Diksmuide (De Watergroep)	≤ 5 m	75 days	no	36
Kluizen I (De Watergroep)	11.5 m	107 days	yes	22
Kluizen II (De Watergroep)	11 m	75	yes	16
De Gijster (Evides)	≤ 27 m on average 13 m	11 weeks		14
Honderdendertig (Evides)	≤ 27 m on average 15 m	ca. 4 weeks	no	19
Petrusplaat (Evides)	≤ 15 m on average 13 m	ca. 4 weeks	no	22
Braakman Spaarbekken 1 (Evides)	≤ 11.2 m on average 10.5 m	ca. 6 weeks	no	100
Berenplaat (Evides)	≤ 6.5 m on average 6 m	1 month (Lucassen et al. 2008)	no	12
WPJ (PWN)	≤ 5.3 m on average 3.9 m	28 – 39 days	yes	20
PSA (PWN)	≤ 12 m on average 21 m	30 – 43 days	yes	4
Afgedamde Maasbekken	3 – 10 m	6 weeks	yes	14

In this table a theoretical degradation potential is estimated. The actual degradation potential will depend on several parameters:

- The OMP composition. Some compounds can be degraded via an oxidative pathway, whereas for others it is very difficult to oxidize them.
- Water quality. Here the concentration and composition of NOM can play a crucial role, but also the pH, nitrate and carbonate concentrations can be very important. It is e.g. known that carbonate is a radical scavenger.
- Light penetration depth. For the Afgedamde Maas it is < 10 cm at the dosing point of iron. This area extends to a few hundred meters in summer, but to some kilometers in winter. WML uses a dosing area of 400 m, in which the color of the water turns to reddish brown, but in the main reservoir the penetration depth for visible light is several meters (it's not clear, however, how large the penetration depth for UV-radiation would be).
- The variation in residence time. This not only varies from one reservoir to another, but also the residence time in one reservoir will not be constant.

- The variation in depth. For the estimation the average depth was taken into account, but from the data it can be concluded that there is a large variation, and in deeper water photo-Fenton processes will be more difficult.
- Variation in mixing conditions. These may affect the degradation of the compounds, as they determine how long and how often a part of the water is lighted.
- Seasonal variations. It has been shown that the degradation of compounds will vary over the year. This can be due to variations in water quality, but also in the intensity of the sunlight.
- Iron concentrations. There probably is an optimum iron dosage, based on one hand on causing an acceptable decrease in light penetration depth and on the other hand offering sufficient reactive surface area.

However, even though many aspects still are unclear, from the literature study and the data in table 2 it can be concluded that oxidative degradation of OMPs under the influence of sunlight may be possible, and in some reservoirs even may significantly contribute to the total degradation of OMPs. Moreover, this affect may be enhanced by the addition of iron to the water which is not included in the numbers in table 2. It certainly is worthwhile to determine to which extent this process can be applied for the removal of OMPs in reservoirs.

Often the presence of iron can be observed in surface water, sometimes as very small particles. In the dosing area of WML the residence time of the water is about 10 hours. Precipitation takes place in a reservoir with a residence time of one week, where probably iron still will be present in the water. Some of the iron, however, will reach the main reservoir, with a residence time of 1,5-2 years. Since 1-2 years  $\text{FeCl}_3$  is being dosed (80% of which precipitates), but so far iron concentrations in the reservoir have not been measured, and neither are data available on OMP degradation in the reservoir since that time. It would be interesting to measure the effect of the iron chloride dosing on the OMP concentrations in the reservoir.

### 3.2 The reductive pathway

The production of electrons on the surface of the Fe(III) bearing mineral controls the potential breakdown of OMP in the reductive pathway. This production is correlated with the Fe(II) concentration in the groundwater that sorbs on the surface of the Fe(III) particle and the rate of heterogeneous oxidation of the Fe(II).

Rates of heterogeneous Fe(II) oxidation under circumneutral pH condition are typical in the order of minutes. This means that the Fe(II) concentration in the groundwater controls the electron production. Let's assume a Fe(II) concentration in the groundwater of 10 mg/L and that the oxidation under low oxygen concentrations is finished within one day. This results in an electron production rate of 178  $\mu\text{M}/\text{day}$ . Next, let's assume that 10% of the produced electrons is available for OMP reduction and 1  $\mu\text{M}$  electron attacks 1  $\mu\text{g}$  of OMP. If similar to the previous example 1  $\mu\text{g}/\text{L}$  of OMP present in the water, and 90% has to be removed, which is 0.9  $\mu\text{g}/\text{L}$ , This would, in this example, take about 1.2 hours.

Dunea has noticed OMP degradation during dune passage, but it is assumed that this is caused by biological processes. WML could not observe reduction of OMPs from groundwater sources (except for the effect of aeration).

### 3.3 Research questions

The main questions for further research based on the present findings are:

1. What is the effect of Fenton like reactions on the OMP concentrations, both in surface water and in groundwater?
2. What is the effect of the dosing of iron on the iron concentration in the water? And does extra dosing of iron also affect the phosphate concentration in the water?
3. What is the effect of iron dosing on the penetration depth for (UV) light?

In order to answer these questions, two routes can be followed:

1. Measuring actual data in groundwater and reservoirs
2. Doing laboratory experiments under well-defined conditions

As fluctuations in reservoirs can be very large, and large differences in residence time occur, it is advised to start with laboratory measurements, to determine the magnitude of the effect of iron redox cycling on the degradation of OMPs that may be expected.

## 4 Conclusions

In this literature study we examined the role of iron redox cycling in micropollutant removal from water. Iron redox cycling occurs at different stages in the drinking water production. The effect on micropollutant removal has had little attention so far.

This study revealed two pathways that are relevant for the drinking water sector where iron redox cycling may have a positive effect on micropollutant removal:

1. **The oxidative pathway.** Iron dosing in surface water reservoirs for phosphate removal may also result in micropollutant removal due to generation of reactive oxygen species (ROS) in sunlit natural waters. Production of Fe(II) by photo-induced reduction of Fe(III) and photo-induced production of H<sub>2</sub>O<sub>2</sub>, both in the presence of DOC, results in the formation of the OH• radical (the photo-Fenton process). The OH• radical is capable for degrading several types of organic component including many micropollutants. Iron(III) dosing in surface water reservoirs might have a positive effect on the photo-Fenton process because the freshly formed Fe(III) precipitates in the surface water are relatively easily photo reducible and this likely results in high turnover rates of Fe(III) to Fe(II) and vice versa. In case of iron dosing by FeSO<sub>4</sub>, oxidation of the added Fe(II) results in an additional source of ROS that might be available for micropollutant removal.
2. **The reductive pathway.** Subsurface iron removal (SIR) results in hydrogeochemical environments around groundwater production wells, that are typically rich in Fe(III) bearing minerals and Fe(II) sorbed on the surface of these precipitates from the anoxic groundwater with high dissolved Fe(II) concentrations. Such an environment is favorable for reduction of oxidized micropollutants due to electron transfer during heterogeneous oxidation of Fe(II) towards contaminant species that approach the surface of the Fe(III) bearing minerals. This results in a chemically reduced contaminant.

This literature survey revealed that both processes occur in the natural environment. Next, the question arises if this may have a significant effect on micropollutant removal. For the reductive pathway at subsurface iron removal sites this is likely the case as these systems are rich in Fe(III) bearing minerals and sorbed Fe(II). There are already indications from a drinking water production site of Vitens that groundwater wells with SIR show degradation of certain oxidized pesticides (personal communication Ron Jong, winning Dinxperlo). However, the removal of micropollutants until now has not yet been related to this process. In addition, degradation reactions of various contaminants in such systems have never been quantified until now.

The significance of iron redox cycling in surface water reservoirs with iron dosing on micropollutant removal is not known. Steady state concentrations of Fe(II) are likely low (in order of magnitude of nM). It is not known if the production of the OH• radicals (in M/hr) is high enough to significantly contribute to contaminant degradation. On the other hand, some species show degradation in certain surface water reservoirs and it has never been investigated if this degradation can be attributed to photo-Fenton like processes in the surface water.

Reductive degradation of contaminants likely also occurs at other redox transition zones in the natural environment. A typical example of such an environment is the groundwater-surface water interface where Fe(II) bearing groundwater oxidizes during exfiltration into surface water resulting in the ubiquitous presence of Fe(III)

precipitates. Zones with high contents of Fe(III) precipitates have been found below drainage ditches and in a ring around subsurface tube drains. Such zones might have a positive effect on the degradation of pesticides and/or veterinary medicines and therefore reduce the surface water load of diffuse contaminants from groundwater. However, these processes in the groundwater-surface water interface have never been subject of study. More insight in these processes is relevant for management of surface water quality, which is also of interest for the drinking water sector.

## 5 References

- Andrews, S.S., Caron, S. and Zafiriou, O.C. (2000) Photochemical oxygen consumption in marine waters: A major sink for colored dissolved organic matter? *Limnology and Oceanography* 45(2), 267-277.
- Batista, A.P.S., Teixeira, A.C.S.C., Cooper, W.J. and Cottrell, B.A. (2016) Correlating the chemical and spectroscopic characteristics of natural organic matter with the photodegradation of sulfamerazine. *Water Research* 93, 20-29.
- Bertelkamp, C., Hofman-Caris, C.H.M., Siegers, W.G., Verschoor, A.M., Hootsmans, M.J.M. and Wols, B.A. (2020) Verkenning zuiveringseffect van bekkens, KWR Water Research Institute, Nieuwegein.
- Bodhipaksha, L.C., Sharpless, C.M., Chin, Y.-P. and MacKay, A.A. (2017) Role of effluent organic matter in the photochemical degradation of compounds of wastewater origin. *Water Research* 110, 170-179.
- Buchholz, A., Laskov, C. and Haderlein, S.B. (2011) Effects of zwitterionic buffers on sorption of ferrous iron at goethite and its oxidation by  $\text{CCl}_4$ . *Environmental Science & Technology* 45(8), 3355-3360.
- Calisto, V., Domingues, M.R.M. and Esteves, V.I. (2011) Photodegradation of psychiatric pharmaceuticals in aquatic environments – Kinetics and photodegradation products. *Water Research* 45(18), 6097-6106.
- Catrouillet, C., Davranche, M., Dia, A., Bouhnik-Le Coz, M., Marsac, R., Pourret, O. and Gruau, G. (2014) Geochemical modeling of Fe(II) binding to humic and fulvic acids. *Chemical Geology* 372, 109-118.
- Chen, Y., Liu, L., Su, J., Liang, J., Wu, B., Zuo, J. and Zuo, Y. (2017) Role of humic substances in the photodegradation of naproxen under simulated sunlight. *Chemosphere* 187, 261-267.
- Cooper, W.J. and Zika, R.G. (1983) Photochemical formation of hydrogen peroxide in surface and ground waters exposed to sunlight. *Science* 220(4598), 711-712.
- Cooper, W.J., Zika, R.G., Petasne, R.G. and Plane, J.M.C. (1988) Photochemical formation of  $\text{H}_2\text{O}_2$  in natural waters exposed to sunlight. *Environmental Science and Technology* 22(10), 1156-1160.
- Du, Q., Jia, W., Dai, J., Du, C., Shao, A., Zhang, R. and Ji, Y. (2020) Effect of dissociation constant ( $\text{pK}_a$ ) of natural organic matter on photo-generation of reactive oxygen species (ROS). *Journal of Photochemistry and Photobiology A: Chemistry* 391.
- Elsner, M., Schwarzenbach, R.P. and Haderlein, S.B. (2004) Reactivity of Fe(II)-bearing minerals toward reductive transformation of organic contaminants. *Environmental Science & Technology* 38(3), 799-807.
- Farley, K.J., Dzombak, D.A. and Morel, F.M. (1985) A surface precipitation model for the sorption of cations on metal oxides. *Journal of Colloid and Interface Science* 106(1), 226-242.
- Fritzsche, A., Bosch, J., Rennert, T., Heister, K., Braunschweig, J., Meckenstock, R.U. and Totsche, K.U. (2012) Fast microbial reduction of ferrihydrite colloids from a soil effluent. *Geochimica et Cosmochimica Acta* 77, 444-456.
- Garg, S., Ito, H., Rose, A.L. and Waite, T.D. (2013a) Mechanism and kinetics of dark iron redox transformations in previously photolyzed acidic natural organic matter solutions. *Environmental Science and Technology* 47(4), 1861-1869.
- Garg, S., Jiang, C. and David Waite, T. (2015) Mechanistic insights into iron redox transformations in the presence of natural organic matter: Impact of pH and light. *Geochimica et Cosmochimica Acta* 165, 14-34.
- Garg, S., Jiang, C., Miller, C.J., Rose, A.L. and Waite, T.D. (2013b) Iron redox transformations in continuously photolyzed acidic solutions containing natural organic matter: Kinetic and mechanistic insights. *Environmental Science and Technology* 47(16), 9190-9197.
- Garg, S., Jiang, C. and Waite, T.D. (2018) Impact of pH on Iron Redox Transformations in Simulated Freshwaters Containing Natural Organic Matter. *Environmental Science and Technology* 52(22), 13184-13194.
- Gault, A.G., Ibrahim, A., Langley, S., Renaud, R., Takahashi, Y., Boothman, C., Lloyd, J.R., Clark, I.D., Ferris, F.G. and Fortin, D. (2011) Microbial and geochemical features suggest iron redox cycling within bacteriogenic iron oxide-rich sediments. *Chemical Geology* 281(1), 41-51.
- Häkkinen, P.J., Anesio, A.M. and Granéli, W. (2004) Hydrogen peroxide distribution, production, and decay in boreal lakes. *Canadian Journal of Fisheries and Aquatic Sciences* 61(8), 1520-1527.

- Hartenbach, A., Hofstetter, T.B., Berg, M., Bolotin, J. and Schwarzenbach, R.P. (2006) Using nitrogen isotope fractionation to assess abiotic reduction of nitroaromatic compounds. *Environmental Science & Technology* 40(24), 7710-7716.
- Henneberry, Y.K., Kraus, T.E.C., Nico, P.S. and Horwath, W.R. (2012) Structural stability of coprecipitated natural organic matter and ferric iron under reducing conditions. *Organic Geochemistry* 48, 81-89.
- Herrmann, M., Menz, J., Olsson, O. and Kümmerer, K. (2015) Identification of phototransformation products of the antiepileptic drug gabapentin: Biodegradability and initial assessment of toxicity. *Water Research* 85, 11-21.
- Jung, H.J., Hong, J.S. and Suh, J.K. (2013) A comparison of fenton oxidation and photocatalyst reaction efficiency for humic acid degradation. *Journal of Industrial and Engineering Chemistry* 19(4), 1325-1330.
- Karlsson, T. and Persson, P. (2012) Complexes with aquatic organic matter suppress hydrolysis and precipitation of Fe(III). *Chemical Geology* 322-323, 19-27.
- Kim, H.B., Kim, J.G., Kim, S.H., Kwon, E.E. and Baek, K. (2019) Consecutive reduction of Cr(VI) by Fe(II) formed through photo-reaction of iron-dissolved organic matter originated from biochar. *Environmental Pollution* 253, 231-238.
- Klausen, J., Troeber, S.P., Haderlein, S.B. and Schwarzenbach, R.P. (1995) Reduction of substituted nitrobenzenes by Fe (II) in aqueous mineral suspensions. *Environmental Science & Technology* 29(9), 2396-2404.
- Kügler, S., Cooper, R.E., Wegner, C.E., Mohr, J.F., Wichard, T. and Küsel, K. (2019) Iron-organic matter complexes accelerate microbial iron cycling in an iron-rich fen. *Science of the Total Environment* 646, 972-988.
- Kulkarni, H.V., Mladenov, N., McKnight, D.M., Zheng, Y., Kirk, M.F. and Nemergut, D.R. (2018) Dissolved fulvic acids from a high arsenic aquifer shuttle electrons to enhance microbial iron reduction. *Science of the Total Environment* 615, 1390-1395.
- Lee, Y.P., Fujii, M., Kikuchi, T., Terao, K. and Yoshimura, C. (2017) Variation of iron redox kinetics and its relation with molecular composition of standard humic substances at circumneutral pH. *PLoS ONE* 12(4).
- Liu, W., Sutton, N.B., Rijnaarts, H.H.M. and Langenhoff, A.A.M. (2020) Anaerobic biodegradation of pharmaceutical compounds coupled to dissimilatory manganese (IV) or iron (III) reduction. *Journal of Hazardous Materials* 388, 119361.
- Lucassen, E., Castellijns, H., Wagenvoort, A. and Smolders, A. (2008) Oorzaken en oplossing interne eutrofiering in spaarbekken de Braakman, pp. 33-36, KNW.
- Marchetti, G., Minella, M., Maurino, V., Minero, C. and Vione, D. (2013) Photochemical transformation of atrazine and formation of photointermediates under conditions relevant to sunlit surface waters: Laboratory measures and modelling. *Water Research* 47(16), 6211-6222.
- Marchisio, A., Minella, M., Maurino, V., Minero, C. and Vione, D. (2015) Photogeneration of reactive transient species upon irradiation of natural water samples: Formation quantum yields in different spectral intervals, and implications for the photochemistry of surface waters. *Water Research* 73, 145-156.
- Méndez-Arriaga, F., Esplugas, S. and Giménez, J. (2010) Degradation of the emerging contaminant ibuprofen in water by photo-Fenton. *Water Research* 44(2), 589-595.
- Meunier, L., Laubscher, H., Hug, S.J. and Sulzberger, B. (2005) Effects of size and origin of natural dissolved organic matter compounds on the redox cycling of iron in sunlit surface waters. *Aquatic Sciences* 67(3), 292-307.
- Mohatt, J.L., Hu, L., Finneran, K.T. and Strathmann, T.J. (2011) Microbially mediated abiotic transformation of the antimicrobial agent sulfamethoxazole under iron-reducing soil conditions. *Environmental Science and Technology* 45(11), 4793-4801.
- Mostafa, S. and Rosario-Ortiz, F.L. (2013) Singlet oxygen formation from wastewater organic matter. *Environmental Science and Technology* 47(15), 8179-8186.
- Nichela, D.A., Donadelli, J.A., Caram, B.F., Haddou, M., Rodriguez Nieto, F.J., Oliveros, E. and García Einschlag, F.S. (2015) Iron cycling during the autocatalytic decomposition of benzoic acid derivatives by Fenton-like and photo-Fenton techniques. *Applied Catalysis B: Environmental* 170-171, 312-321.
- Rosso, K.M., Smith, D.M. and Dupuis, M. (2003) An ab initio model of electron transport in hematite ( $\alpha$ -Fe<sub>2</sub>O<sub>3</sub>) basal planes. *The Journal of chemical physics* 118(14), 6455-6466.
- Samperio-Ramos, G., González-Dávila, M. and Santana-Casiano, J.M. (2018) Impact on the Fe redox cycling of organic ligands released by *Synechococcus* PCC 7002, under different iron fertilization scenarios. Modeling approach. *Journal of Marine Systems* 182, 67-78.
- Schaefer, M.V., Gorski, C.A. and Scherer, M.M. (2011) Spectroscopic evidence for interfacial Fe (II)- Fe (III) electron transfer in a clay mineral. *Environmental Science & Technology* 45(2), 540-545.

- Sivey, J.D. and Roberts, A.L. (2012) Abiotic reduction reactions of dichloroacetamide safeners: Transformations of "inert" agrochemical constituents. *Environmental Science and Technology* 46(4), 2187-2195.
- Southworth, B.A. and Voelker, B.M. (2003) Hydroxyl radical production via the photo-fenton reaction in the presence of fulvic acid. *Environmental Science and Technology* 37(6), 1130-1136.
- Strathmann, T.J. and Stone, A.T. (2003) Mineral surface catalysis of reactions between FeII and oxime carbamate pesticides. *Geochimica et Cosmochimica Acta* 67(15), 2775-2791.
- Strehlau, J. (2016) Contaminant reduction by iron oxide nanoparticles: Environmental variables and evolving reactivity.
- Stumm, W. (1987) *Aquatic surface chemistry: Chemical processes at the particle-water interface*, John Wiley & Sons.
- Sur, B., De Laurentiis, E., Minella, M., Maurino, V., Minero, C. and Vione, D. (2012) Photochemical transformation of anionic 2-nitro-4-chlorophenol in surface waters: Laboratory and model assessment of the degradation kinetics, and comparison with field data. *Science of the Total Environment* 426, 296-303.
- Vandenbohede, A., Wallis, I. and Alleman, T. (2019) Trace metal behavior during in-situ iron removal tests in Leuven, Belgium. *Science of The Total Environment* 648, 367-376.
- Vermilyea, A.W. and Voelker, B.M. (2009) Photo-fenton reaction at near neutral pH. *Environmental Science and Technology* 43(18), 6927-6933.
- Vione, D., Minella, M., Maurino, V. and Minero, C. (2014) Indirect photochemistry in sunlit surface waters: Photoinduced production of reactive transient species. *Chemistry - A European Journal* 20(34), 10590-10606.
- Voelker, B.M., Morel, F.M.M. and Sulzberger, B. (1997) Iron redox cycling in surface waters: Effects of humic substances and light. *Environmental Science and Technology* 31(4), 1004-1011.
- Voelker, B.M. and Sedlak, D.L. (1995) Iron reduction by photoproduced superoxide in seawater. *Marine Chemistry* 50(1-4), 93-102.
- Wang, K., Garg, S. and Waite, T.D. (2017) Light-Mediated Reactive Oxygen Species Generation and Iron Redox Transformations in the Presence of Exudate from the Cyanobacterium *Microcystis aeruginosa*. *Environmental Science and Technology* 51(15), 8384-8395.
- Williams, A.G. and Scherer, M.M. (2004) Spectroscopic evidence for Fe (II)– Fe (III) electron transfer at the iron oxide– water interface. *Environmental Science & Technology* 38(18), 4782-4790.
- Wordofa, D.N., Adhikari, D., Dunham-Cheatham, S.M., Zhao, Q., Poulson, S.R., Tang, Y. and Yang, Y. (2019) Biogeochemical fate of ferrihydrite-model organic compound complexes during anaerobic microbial reduction. *Science of the Total Environment* 668, 216-223.
- Xing, G., Garg, S. and David Waite, T. (2019) Is Superoxide-Mediated Fe(III) Reduction Important in Sunlit Surface Waters? *Environmental Science and Technology* 53(22), 13179-13190.
- Zepp, R.G., Faust, B.C. and Jürg, H. (1992) Hydroxyl Radical Formation in Aqueous Reactions (pH 3-8) of Iron(II) with Hydrogen Peroxide: The Photo-Fenton Reaction. *Environmental Science and Technology* 26(2), 313-319.

# I Kinetic data for Fe redox cycling in literature

Table 3: Kinetic model for Fe redox cycling on continuous photolysis of pH 4 SRFA (Suwannee River Fulvic Acids) solutions (Garg et al. 2013b)

Table 1. Kinetic Model for Fe Redox Cycling on Continuous Photolysis of pH 4 SRFA Solutions.

no.	reaction	model value	published value	reference
light-mediated reactions				
1	SRFA + $h\nu$ → SRFA*	calculated		
	SRFA* + $^3\text{O}_2$ → SRFA + $^1\text{O}_2$	$\Phi \approx 0.5\%$	$\Phi \approx 0.5\%$	Paul et al. <sup>35</sup>
2	$^1\text{O}_2 \xrightarrow{\text{H}_2\text{O}} ^3\text{O}_2$	$2.4 \times 10^5 \text{ s}^{-1a}$	$2.4 \times 10^5 \text{ s}^{-1}$	Dalrymple, et al. <sup>36</sup>
3	$\text{Q} + h\nu \xrightarrow{k_t} \text{Q}^- \xrightarrow{k_d} \text{NRP}^b$	$k_t = 10 \times 10^{-5} \text{ s}^{-1e}; k_d = 5.8 \times 10^3 \text{ s}^{-1}$		5
4	$\text{Q}^- + ^3\text{O}_2 \xrightarrow{\text{H}^+} \text{Q} + \text{HO}_2^*$	$\sim 1 \times 10^9 \text{ M}^{-1}\text{s}^{-1}$	$1 \times 10^9 \text{ M}^{-1}\text{s}^{-1}$	5
5	$\text{A}^{2-} + \text{HO}_2^* \xrightarrow{\text{H}^+} \text{A}^- + \text{H}_2\text{O}_2$	$2 \times 10^5 \text{ M}^{-1}\text{s}^{-1d}$	$\sim 1 \times 10^5 \text{ M}^{-1}\text{s}^{-1}$	37
6	$\text{A}^- + \text{HO}_2^* \rightarrow \text{A}^{2-} + \text{O}_2$	$3 \times 10^5 \text{ M}^{-1}\text{s}^{-1}$	$2.5 \times 10^5 \text{ M}^{-1}\text{s}^{-1}$	5
7	$\text{A}^- + ^1\text{O}_2 \xrightarrow{\text{H}^+} \text{A} + \text{HO}_2^*$	$1.0 \times 10^8 \text{ M}^{-1}\text{s}^{-1}$	$1.5 \times 10^8 \text{ M}^{-1}\text{s}^{-1}$	5
8	$\text{HO}_2^* + \text{HO}_2^* \rightarrow \text{O}_2 + \text{H}_2\text{O}_2$	$1.1 \times 10^7 \text{ M}^{-1}\text{s}^{-1}$	$1.1 \times 10^7 \text{ M}^{-1}\text{s}^{-1}$	11
9	$\text{R} + h\nu \rightarrow \text{R}^*$	$6 \times 10^{-6} \text{ s}^{-1e}$	$7.5 \times 10^{-6} \text{ s}^{-1}$	31
10	$\text{R}^* + \text{HO}_2^* \rightarrow \text{R}^- + \text{O}_2 + \text{H}^+$	$1.5 \times 10^5 \text{ M}^{-1}\text{s}^{-1}$	$10^4\text{--}10^9 \text{ M}^{-1}\text{s}^{-1}$	24
11	$\text{R}^* + \text{R}^* \rightarrow \text{R} - \text{R}$	$1.0 \times 10^3 \text{ M}^{-1}\text{s}^{-1}$	$1.0 \times 10^3 \text{ M}^{-1}\text{s}^{-1}$	31
12	$\text{R} + h\nu \xrightarrow{\text{O}_2, \text{HO}_2^*} \text{RO}_2^*$	$1 \times 10^{-6} \text{ s}^{-1e,f}$		this work
13	$\text{RO}_2^* + \text{RO}_2^* \rightarrow \text{RO}_4\text{R}$	$1.0 \times 10^6 \text{ M}^{-1}\text{s}^{-1}$	$10^5\text{--}10^6 \text{ M}^{-1}\text{s}^{-1}$	38
14	$\text{RO}_2^* \rightarrow \text{R}^{*+} + \text{HO}_2^*$	$1 \times 10^{-2} \text{ s}^{-1f}$	$< 3 \text{ s}^{-1}$	38
Fe(II) oxidation and Fe(III) reduction reactions				
15	$\text{Fe(II)} + \text{A}^- \rightarrow \text{Fe(III)} + \text{A}^{2-}$	$1 \times 10^5 \text{ M}^{-1}\text{s}^{-1}$	$1 \times 10^5 \text{ M}^{-1}\text{s}^{-1}$	5
16	$\text{Fe(III)} + \text{A}^{2-} \rightarrow \text{Fe(II)} + \text{A}^-$	$4 \times 10^3 \text{ M}^{-1}\text{s}^{-1}$	$4 \times 10^3 \text{ M}^{-1}\text{s}^{-1}$	5
17	$\text{Fe(II)} + \text{RO}_2^* \rightarrow \text{Fe(III)} + \text{RO}_2\text{H}$	$1 \times 10^7 \text{ M}^{-1}\text{s}^{-1f}$	$10^5\text{--}10^7 \text{ M}^{-1}\text{s}^{-1}$	13
18	$\text{Fe(III)} \xrightarrow{h\nu, \text{L}} \text{Fe(II)} + \text{L}_{\text{ox}}$	$7.5 \times 10^{-3} \text{ s}^{-1f}$		this work
19	$\text{Fe(II)} + \text{HO}_2^* \rightarrow \text{Fe(III)} + \text{H}_2\text{O}_2$	$2.4 \times 10^6 \text{ M}^{-1}\text{s}^{-1}$	$2.4 \times 10^6 \text{ M}^{-1}\text{s}^{-1}$	26
20	$\text{Fe(III)} + \text{HO}_2^* \rightarrow \text{Fe(II)} + \text{O}_2$	$2.0 \times 10^5 \text{ M}^{-1}\text{s}^{-1}$	$(2.8\text{--}5) \times 10^5 \text{ M}^{-1}\text{s}^{-1}$	39

<sup>a</sup>Rate constant is  $1.6 \times 10^4 \text{ s}^{-1}$  in  $\text{D}_2\text{O}$  solution.<sup>40</sup> <sup>b</sup>NRP represents nonreactive product. <sup>c</sup>Pseudofirst order rate constant based on  $[\text{Q}]_{\text{T}} = 1.3 \text{ mmol}\cdot\text{g}^{-1}$  SRFA where Q represents electron accepting quinone moieties in humic and fulvic acids.<sup>41</sup> <sup>d</sup>Based on  $[\text{A}]_{\text{T}} = 35.4 \text{ }\mu\text{mol}\cdot(\text{g SRFA})^{-1}$  where  $\text{A}^{2-}$  represents the reduced hydroquinone-like species which occurs natively in SRFA but contributes only to a very small portion of the overall electron donating capacity of humic and fulvic acids (phenolic moieties are the main electron donating groups in SRFA.<sup>42</sup>) <sup>e</sup>Pseudofirst order rate constant based on  $[\text{R}]_{\text{T}} = 44 \text{ mmol}\cdot\text{g}^{-1}$  SRFA;<sup>31</sup> R represents the bulk organic concentration in SRFA. <sup>f</sup>Based on best-fit model results.

Table 4: calculated values of  $k_1/k_2$  Fe(III) reductant concentration and Fe(II) oxidant concentration (Garg et al. 2013a)

Table 1. Calculated Values of  $k_1/k_2$ , Fe(III) Reductant Concentration and Fe(II) Oxidant Concentration

[SRFA] (mg·L <sup>-1</sup> )	[Fe] <sub>0</sub> (nM)	[Fe(II)] <sub>ss</sub> (nM)	$k_1/k_2$	[A <sup>2-</sup> ] <sub>0</sub> (nM)	[A <sup>2-</sup> ] <sub>0</sub> (μmol·g <sup>-1</sup> )	[A <sup>-</sup> ] <sub>0</sub> (nM)	[A <sup>-</sup> ] <sub>0</sub> (μmol·g <sup>-1</sup> )
Fe(III) Reduction in Nonphotolyzed SRFA Solution							
10.0	100.0	29.3	0.037	354.5	35.5	0	0
	50.0	19.5					
5.0	100.0	22.5	0.042	176.8	35.4	0	0
	50.0	15.4					
	25.0	8.6					
Fe(II) Oxidation in Photolyzed SRFA Solution							
10.0	100.0	29.9	0.04	267.6	26.7	86.6	8.7
	50.0	10.4					
5.0	100.0	60.3		133.0	26.6	44.3	8.9
	2.5	78.6					
1.0	100.0	94.2		29.6	29.6	5.9	5.9
Fe(III) Reduction in Photolyzed SRFA Solution							
10.0	100.0	9.0	0.04	261.4	26.1	93.2	9.3
	50.0	4.5					
5.0	100.0	13.9		156.1	31.2	21.2	4.2
	50.0	6.4					
	25.0	2.5					

Table 5: kinetic model for generation of Fe(II) oxidant on photolysis of SRFA at pH 4 (Garg et al. 2013a)

Table 2. Kinetic Model for Generation of Fe(II) Oxidant on Photolysis of SRFA at pH 4

no.	reaction	model value	published value	reference
Light-mediated Reactions				
1	SRFA+hν→SRFA*	calculated		
	SRFA* + <sup>3</sup> O <sub>2</sub> → SRFA + <sup>1</sup> O <sub>2</sub>	Φ ~ 0.5%	Φ ~ 0.5%	32
2	<sup>1</sup> O <sub>2</sub> $\xrightarrow{H_2O}$ <sup>2</sup> O <sub>2</sub>	2.4 × 10 <sup>5</sup> s <sup>-1a</sup>	2.4 × 10 <sup>5</sup> s <sup>-1</sup>	33
3	Q + hν $\xrightarrow{k_f}$ Q <sup>-</sup> $\xrightarrow{k_d}$ NRP	k <sub>f</sub> = 6 × 10 <sup>-5</sup> s <sup>-1b</sup> ; k <sub>d</sub> = 5.8 × 10 <sup>3</sup>	-	this work
4	Q <sup>-</sup> + <sup>3</sup> O <sub>2</sub> $\xrightarrow{H^+}$ Q + HO <sub>2</sub> <sup>*</sup>	~1 × 10 <sup>9</sup> M <sup>-1</sup> ·s <sup>-1</sup>	1 × 10 <sup>9</sup> M <sup>-1</sup> ·s <sup>-1</sup>	29
5	HO <sub>2</sub> <sup>*</sup> + HO <sub>2</sub> <sup>*</sup> → H <sub>2</sub> O <sub>2</sub> + O <sub>2</sub>	2 × 10 <sup>6</sup> M <sup>-1</sup> ·s <sup>-1</sup>	2 × 10 <sup>6</sup> M <sup>-1</sup> ·s <sup>-1</sup>	25
6	R + hν → R*	4 × 10 <sup>-6</sup> s <sup>-1c</sup>	7.5 × 10 <sup>-6</sup> s <sup>-1c</sup>	27
7	R* + HO <sub>2</sub> <sup>*</sup> → R <sup>-</sup> + O <sub>2</sub> + H <sup>+</sup>	2.0 × 10 <sup>5</sup> M <sup>-1</sup> ·s <sup>-1</sup>	10 <sup>4</sup> –10 <sup>9</sup> M <sup>-1</sup> ·s <sup>-1</sup>	34
8	R*+R*→R <sub>2</sub>	1.0 × 10 <sup>3</sup> M <sup>-1</sup> ·s <sup>-1</sup>		27
9	A <sup>2-</sup> + HO <sub>2</sub> <sup>*</sup> $\xrightarrow{H^+}$ A <sup>-</sup> + H <sub>2</sub> O <sub>2</sub>	2 × 10 <sup>5</sup> M <sup>-1</sup> ·s <sup>-1d</sup>	~1 × 10 <sup>5</sup> M <sup>-1</sup> ·s <sup>-1</sup>	20
10	A <sup>-</sup> + HO <sub>2</sub> <sup>*</sup> → A <sup>2-</sup> + O <sub>2</sub>	2.5 × 10 <sup>5</sup> M <sup>-1</sup> ·s <sup>-1d</sup>	~ 10k <sub>9</sub>	27
11	A <sup>-</sup> + <sup>1</sup> O <sub>2</sub> $\xrightarrow{H^+}$ A + HO <sub>2</sub> <sup>*</sup>	~1.5 × 10 <sup>8</sup> M <sup>-1</sup> ·s <sup>-1</sup>	diffusion limited	this work
Fe(II) Oxidation and Fe(III) Reduction Reactions Occurring in Dark				
12	Fe(II) + A <sup>-</sup> → Fe(III) + A <sup>2-</sup>	1 × 10 <sup>5</sup> M <sup>-1</sup> ·s <sup>-1e</sup>		this work
13	Fe(III) + A <sup>2-</sup> → Fe(II) + A <sup>-</sup>	k <sub>13</sub> /k <sub>14</sub> = 0.04 <sup>f</sup>		this work

<sup>a</sup>Rate constant is 1.6 × 10<sup>4</sup> s<sup>-1</sup> in D<sub>2</sub>O solution.<sup>26</sup> <sup>b</sup>Pseudo-first order rate constant based on [Q]<sub>T</sub> = 1.7 mmol·g<sup>-1</sup> SRFA;<sup>28</sup> represents an apparent rate constant (see SI-4 for more details). <sup>c</sup>Pseudo-first order rate constant based on [R]<sub>T</sub> = 44 mmol·g<sup>-1</sup> SRFA.<sup>27</sup> <sup>d</sup>Based on best-fit model results. <sup>e</sup>Based on best-fit model results to Fe(II) generation from Fe(III) reduction in nonphotolyzed SRFA solution and Fe(II) decay kinetics in irradiated SRFA solution. <sup>f</sup>Ratio determined based on measured steady-state Fe(II) concentration generated from Fe(III) reduction in nonphotolyzed SRFA solution (see text for more details).

Table 6: Kinetic model for Fe redox transformation in the pH range 6.8 – 8.7 (Garg et al. 2018)

**Table 1. Kinetic Model for Fe Redox Transformation in the pH Range 6.8–8.7**

no.	reaction	rate constant (M <sup>-1</sup> s <sup>-1</sup> )	ref	no.	reaction	rate constant (M <sup>-1</sup> s <sup>-1</sup> )	ref
Generation and Consumption of ROS on Irradiation				Fe(II) Oxidation in Dark			
1	R + hν → R*	calculated <sup>a</sup>		21	Fe(II)' + O <sub>2</sub> → Fe(III)' + O <sub>2</sub> <sup>•-</sup>	log k = -13.77 + 1 2 pH	1
	R* + <sup>3</sup> O <sub>2</sub> → R + <sup>1</sup> O <sub>2</sub>	Φ ~ 0.5%	59	22	Fe(II)L <sub>1</sub> + O <sub>2</sub> → Fe(III)L <sub>1</sub> + O <sub>2</sub> <sup>•-</sup>	log k = -1.83 + 0.48 pH	this work
2	<sup>1</sup> O <sub>2</sub> $\xrightarrow{H_2O}$ <sup>3</sup> O <sub>2</sub>	2.4 × 10 <sup>5</sup> s <sup>-1</sup>	60	23	Fe(II)' + A <sup>-</sup> → Fe(III)' + A <sup>2-</sup>	log k = 4.44 + 0.18 pH	this work
3	Q + hν $\xrightarrow{k_f}$ Q <sup>-</sup> $\xrightarrow{k_d}$ NRP	k <sub>f</sub> = 2.4 × 10 <sup>-4</sup> s <sup>-1b</sup> k <sub>d</sub> = 5.8 × 10 <sup>3</sup> s <sup>-1</sup>	this work, 31	24	Fe(II)L <sub>1</sub> + A <sup>-</sup> → Fe(III)L <sub>1</sub> + A <sup>2-</sup>	log k = 4.44 + 0.18pH	this work
4	Q <sup>-</sup> + O <sub>2</sub> → O <sub>2</sub> <sup>•-</sup> + Q	~1 × 10 <sup>9</sup> M <sup>-1</sup> s <sup>-1</sup>	31	25	Fe(II)' + L <sub>1</sub> $\xrightleftharpoons[k_d]{k_f}$ Fe(II)L <sub>1</sub>	k <sub>f</sub> = 1.4 × 10 <sup>4</sup> ; k <sub>d</sub> = 8.7 × 10 <sup>-3</sup> s <sup>-1</sup>	28
5	O <sub>2</sub> <sup>•-</sup> + O <sub>2</sub> <sup>•-</sup> $\xrightarrow{2H^+}$ O <sub>2</sub> + H <sub>2</sub> O <sub>2</sub>	5 × 10 <sup>12</sup> [H <sup>+</sup> ]	61	26	Fe(II)L <sub>1</sub> $\xrightleftharpoons[slow]{k_{f1}}$ Fe(II)L <sub>2</sub>	6 × 10 <sup>-3</sup> s <sup>-1</sup>	28
6	R + hν → R*	1.5 × 10 <sup>-6</sup> s <sup>-1a</sup>	31	Additional Fe(III) Reduction Pathway in Irradiated Condition			
7	R* + O <sub>2</sub> <sup>•-</sup> → R <sup>-</sup> + O <sub>2</sub>	1–2 × 10 <sup>5</sup> M <sup>-1</sup> s <sup>-1</sup>	31	27	Fe(III)L <sub>1</sub> $\xrightarrow{h\nu}$ Fe(II)' + L <sub>ox</sub>	5–8 × 10 <sup>-3g</sup>	16
8	R* + R* → R <sub>2</sub>	1 × 10 <sup>3</sup> M <sup>-1</sup> s <sup>-1</sup>	31	28	Fe(III)L <sub>2</sub> $\xrightarrow{h\nu}$ Fe(II)' + L <sub>ox</sub>	5–8 × 10 <sup>-4g</sup>	this work
Transformation of Hydroquinone and Semiquinone-Like Moieties on Irradiation				Additional Fe(II) Oxidation Pathway in Irradiated Condition			
9	A <sup>2-</sup> + O <sub>2</sub> <sup>•-</sup> → A <sup>-</sup> + H <sub>2</sub> O <sub>2</sub>	3.4 × 10 <sup>4</sup> M <sup>-1</sup> s <sup>-1c</sup>	31	29	Fe(II)' + RO <sub>2</sub> <sup>•</sup> → Fe(III)' + RO <sub>2</sub> <sup>-</sup>	1 × 10 <sup>7</sup>	62
10	A <sup>-</sup> + O <sub>2</sub> <sup>•-</sup> → A <sup>2-</sup> + O <sub>2</sub>	~10–20k <sub>9</sub>	31	30	Fe(II)L <sub>1</sub> + RO <sub>2</sub> <sup>•</sup> → Fe(III)L <sub>1</sub> + RO <sub>2</sub> <sup>-</sup>	1 × 10 <sup>7</sup>	62
11	A <sup>-</sup> + <sup>1</sup> O <sub>2</sub> → A + O <sub>2</sub> <sup>•-</sup>	~1 × 10 <sup>9</sup> M <sup>-1</sup> s <sup>-1</sup>	31	Fe(II) trapping by FZ			
Generation of Short-Lived Fe(II) Oxidant on Irradiation				31	Fe(II) + 3FZ → Fe(II)FZ <sub>3</sub> <sup>h</sup>	3 × 10 <sup>11i</sup>	63
12	R $\xrightarrow{h\nu}$ RO <sub>2</sub> <sup>•</sup>	5 × 10 <sup>-7</sup> s <sup>-1a</sup>	17	<sup>a</sup> Pseudo-first order rate constant based on [R] <sub>T</sub> = 43 mmol.g <sup>-1</sup> SRFA; <sup>53</sup> R represents the bulk organic concentration in SRFA. <sup>b</sup> Pseudo-first order rate constant based on [Q] <sub>T</sub> = 0.67 mmol.g <sup>-1</sup> SRFA where Q represents electron accepting quinone moieties in humic and fulvic acids as reported earlier. <sup>64</sup> <sup>c</sup> Based on [A] <sub>T</sub> = 35.4 μmol.g <sup>-1</sup> SRFA; <sup>14</sup> rate constant calculated based on the measured pseudo-first order O <sub>2</sub> <sup>•-</sup> decay rate constant in 10 mg.L <sup>-1</sup> SRFA solution. <sup>44</sup> <sup>d</sup> Upper limit used for fitting the pH 6.8 results while lower limit is used for fitting the data at pH 7.3, 8.3 and 8.8. <sup>e</sup> Based on L concentration of 300–400 nmoles.mg <sup>-1</sup> SRFA as determined here (see SI Table S2). <sup>f</sup> Based on L concentration of 1.3 μmoles.mg <sup>-1</sup> SRFA. <sup>g</sup> Increases slightly with decrease in pH as indicated. <sup>h</sup> Fe(II) represents the total Fe(II) including Fe(II)', Fe(II)L <sub>1</sub> and Fe(II)L <sub>2</sub> . <sup>i</sup> reported rate constant for Fe(II)' trapping by FZ.			
13	RO <sub>2</sub> <sup>•</sup> + RO <sub>2</sub> <sup>•</sup> → RO <sub>4</sub> R	1 × 10 <sup>6</sup> M <sup>-1</sup> s <sup>-1</sup>	17				
14	RO <sub>2</sub> <sup>•</sup> → R <sup>•+</sup> + HO <sub>2</sub>	1 × 10 <sup>-2</sup> M <sup>-1</sup> s <sup>-1</sup>	17				
Fe(III) Reduction in Dark							
15	Fe(III)L <sub>1</sub> + A <sup>2-</sup> → Fe(II)L <sub>1</sub> + A <sup>-</sup>	5–7 × 10 <sup>3c,d</sup>	16				
16	Fe(III)L <sub>2</sub> + A <sup>2-</sup> → Fe(II)L <sub>2</sub> + A <sup>-</sup>	1 × 10 <sup>2</sup>	this work				
17	Fe(III)L <sub>1</sub> + A <sup>-</sup> → Fe(II)L <sub>1</sub> + A	3.5 × 10 <sup>4</sup>	this work				
18	Fe(III)L <sub>2</sub> + A <sup>-</sup> → Fe(II)L <sub>2</sub> + A	1 × 10 <sup>3</sup>	this work				
19	Fe(III)' + L <sub>1</sub> $\xrightleftharpoons[k_d]{k_f}$ Fe(III)L <sub>1</sub>	k <sub>f</sub> = 6 × 10 <sup>6e</sup> ; k <sub>d</sub> = 6 × 10 <sup>-5</sup> s <sup>-1</sup>	5				
20	Fe(III)L <sub>1</sub> $\xrightleftharpoons[slow]{k_{f1}}$ Fe(III)L <sub>2</sub>	k <sub>f1</sub> = 6 × 10 <sup>-3</sup> s <sup>-1</sup>	this work				

Table 7: Kinetic model for photochemical Fe(III) reduction at pH 8,3 (Xing et al. 2019)

**Table 1. Kinetic Model for Photochemical Fe(III) Reduction at pH 8.3**

no	reaction	rate constant	ref
Generation and Consumption of ROS on Irradiation			
1	$R \xrightarrow{h\nu} R^*$ $R^* + {}^3O_2 \rightarrow R + {}^1O_2$	$0.5 s^{-1a}$ $\Phi \approx 0.5\%$	74
2	${}^1O_2 \xrightarrow{H_2O} {}^3O_2$	$2.4 \times 10^5 s^{-1}$	75
3	$Q + h\nu \xrightarrow{k_f} Q^- \xrightarrow{k_d} NRP$	$k_f = 2.4 \times 10^{-4} s^{-1b}$ ; $k_d = 5.8 \times 10^3 s^{-1}$	1, 27
4	$Q^- + O_2 \rightarrow O_2^{\bullet-} + Q$	$\sim 1 \times 10^9 M^{-1} s^{-1}$	1
5	$O_2^{\bullet-} + O_2^{\bullet-} \xrightarrow{2H^+} H_2O_2 + O_2$	$8.0 \times 10^4 M^{-1} s^{-1}$	
6	$R + h\nu \rightarrow R^*$	$1.5 \times 10^{-6} s^{-1a}$	1
7	$R^* + O_2^{\bullet-} \rightarrow R^- + O_2$	$1 \times 10^5 M^{-1} s^{-1}$	1
8	$R^* + R^* \rightarrow R_2$	$1 \times 10^3 M^{-1} s^{-1}$	1
SRFA-Catalyzed Superoxide Decay			
9	$A^{2-} + O_2^{\bullet-} \rightarrow A^- + H_2O_2$	$3.4 \times 10^4 M^{-1} s^{-1c}$	27
10	$A^- + O_2^{\bullet-} \rightarrow A^{2-} + O_2$	$\sim 10-20 k_9$	27
11	$A^- + {}^1O_2 \rightarrow A + O_2^{\bullet-}$	$\sim 1 \times 10^9 M^{-1} s^{-1}$	27
Fe(III)L Formation and Transformation on Aging			
12	$Fe(III)' + L \xrightleftharpoons[k_d]{k_f} Fe(III)L$	$k_f = 6 \times 10^6 M^{-1} s^{-1d}$ ; $k_d = 6 \times 10^{-5} s^{-1}$	41
13	$Fe(III)L \xrightleftharpoons[slow]{k_{fl}} Fe(III)L'$	$k_{fl} = 1 \times 10^{-3} s^{-1}$	27
Fe(III)L Reduction in Dark			
14	$Fe(III)L + A^{2-} \rightarrow Fe(II)L + A^-$	$5 \times 10^3 M^{-1} s^{-1c}$	27
15	$Fe(III)L' + A^{2-} \rightarrow Fe(II)L' + A^-$	$1 \times 10^2 M^{-1} s^{-1}$	27
16	$Fe(III)L + A^- \rightarrow Fe(II)L + A$	$3.5 \times 10^4 M^{-1} s^{-1}$	27
17	$Fe(III)L' + A^- \rightarrow Fe(II)L' + A$	$1 \times 10^3 M^{-1} s^{-1}$	27
AFO-L Formation, Dissolution, and Transformation on Aging			
18	$Fe(III)' + Fe(III)' \rightarrow AFO + AFO$	$1.1 \times 10^7 M^{-1} s^{-1}$	49
19	$Fe(III)' + AFO \rightarrow AFO + AFO$	$4 \times 10^6 M^{-1} s^{-1}$	49
20	$AFO \rightarrow Fe(III)'$	$1.0 \times 10^{-3} s^{-1c}$	this work
21	$AFO \rightarrow AFO_{aged}$	$f$	
LMCT-Mediated Fe(III) Reduction in Irradiated Condition			
22	$Fe(III)L \xrightarrow{h\nu} Fe(II)' + L_{ox}$	$6 \times 10^{-3} s^{-1}$	27
23	$Fe(III)L' \xrightarrow{h\nu} Fe(II)' + L_{ox}$	$5 \times 10^{-4} s^{-1}$	27
24	$AFO \xrightarrow{h\nu} Fe(II)'$	$5 \times 10^{-4} s^{-1e}$	this work 62,
25	$Fe(III)' \xrightarrow{h\nu} Fe(II)'$	$2 \times 10^{-3} s^{-1}$	62
SMIR in Irradiated Condition			
26	$Fe(III)' + O_2^{\bullet-} \rightarrow Fe(II)' + O_2$	$1.5 \times 10^8 M^{-1} s^{-1}$	18
27	$Fe(III)L + O_2^{\bullet-} \rightarrow Fe(II)L + O_2$	$2 \times 10^4 M^{-1} s^{-1}$	13, 27
28	$Fe(III)L' + O_2^{\bullet-} \rightarrow Fe(II)L' + O_2$	$\ll 2 \times 10^4 M^{-1} s^{-1}$	this work
Fe(II) trapping by FZ			
29	$Fe(II) + 3FZ \rightarrow Fe(II)FZ_3^g$	$3 \times 10^{11} M^{-3} s^{-1h}$	76

<sup>a</sup>R represents the bulk organic concentration in SRFA;  $[R]_T = 43 \text{ mmol g}^{-1}$  SRFA. <sup>b</sup>Pseudo-first-order rate constant based on  $[Q]_T = 0.67 \text{ mmol g}^{-1}$  SRFA, where Q represents electron-accepting quinone moieties in humic and fulvic acids as reported earlier. <sup>c</sup>Based on  $[A]_T = 35.4 \text{ } \mu\text{mol g}^{-1}$  SRFA; <sup>d</sup>rate constant calculated based on the measured pseudo-first-order  $O_2^{\bullet-}$  decay rate constant in  $10.0 \text{ mg L}^{-1}$  SRFA solution. <sup>e</sup>Based on L concentration of  $32.0 \text{ nmol mg}^{-1}$  SRFA as reported earlier. <sup>f</sup>The rate constant decreases with aging of AFO; this represents the value for fresh AFO particles; varies for AFO and AFO-L. <sup>g</sup>The aging of AFO varies on the solution conditions. <sup>h</sup>Fe(II) represents the total Fe(II) including Fe(II)', Fe(II)L, and Fe(II)L'. <sup>h</sup>Reported rate constant for Fe(II)' trapping by FZ.

Table 8: iron (Fe) redox rate constants and steady-state Fe(II) fraction for each standard HS (humic substances) samples (Lee et al. 2017)

Table 1. Iron (Fe) redox rate constants and steady-state Fe(II) fraction ( $[\text{Fe(II)}]_{\text{ss}}/[\text{Fe}]_{\text{T}}$ ) for each standard HS samples.

Code of SHS	$k_{\text{O}_2}$ ( $\text{M}^{-1} \text{s}^{-1}$ )		$k_{\text{H}_2\text{O}_2}$ ( $\times 10^3 \text{M}^{-1} \text{s}^{-1}$ )		$k_{\text{red}_d}$ ( $\times 10^{-6} \text{s}^{-1}$ )		$k_{\text{red}_p}$ ( $\times 10^{-5} \text{s}^{-1}$ )		$[\text{Fe(II)}]_{\text{ss}}/[\text{Fe}]_{\text{T}}$ (%), dark		$[\text{Fe(II)}]_{\text{ss}}/[\text{Fe}]_{\text{T}}$ , light	
	pH 8.0	pH 7.0	pH 8.0	pH 7.0	pH 8.0	pH 7.0	pH 8.0	pH 7.0	pH 8.0	pH 7.0	pH 8.0	pH 7.0
2S101H	31.4 (1.6)	6.13 (1.73)	41.0 (11.0)	6.51 (0.93)	9.02 (0.68)	18.1 (1.8)	8.20 (1.97)	36.8 (14.1)	0.0941 (0.0793–0.112)	0.996 (0.715–1.47)	0.942 (0.668–1.27)	17.7 (9.72–28.3)
1S102H	17.4 (1.9)	5.57 (0.28)	7.11 (5.08)	1.18 (0.62)	5.63 (1.26)	16.5 (0.9)	39.4 (1.2)	50.5 (3.1)	0.124 (0.0830–0.180)	1.17 (1.03–1.33)	8.09 (6.85–9.74)	27.2 (24.7–29.9)
1S103H	22.4 (1.9)	8.05 (1.12)	19.7 (5.8)	3.52 (0.32)	8.60 (0.27)	12.3 (0.0)	3.96 (0.73)	35.6 (5.2)	0.135 (0.117–0.158)	0.579 (0.509–0.670)	0.753 (0.568–0.986)	14.9 (11.7–18.7)
1S104H	22.4 (1.9)	6.62 (1.23)	8.62 (6.24)	2.94 (0.36)	9.68 (3.60)	15.7 (0.7)	22.9 (3.2)	53.0 (3.5)	0.166 (0.0922–0.262)	0.899 (0.728–1.14)	3.94 (2.99–5.15)	23.9 (20.0–29.0)
1R103H	27.2 (2.4)	7.55 (1.90)	19.7 (5.8)	3.09 (0.20)	7.83 (0.18)	(n.m.)	(n.m.)	(n.m.)	0.104 (0.0912–0.120)	(n.a.)	(n.a.)	(n.a.)
1R105H	29.5 (5.2)	7.20 (2.22)	20.5 (5.6)	5.27 (0.74)	9.16 (0.07)	25.8 (2.5)	6.07 (1.08)	33.1 (0.5)	0.113 (0.0940–0.140)	1.28 (0.901–1.95)	0.853 (0.607–1.21)	15.2 (12.0–20.4)
1R107H	19.9 (4.7)	10.6 (2.7)	49.8 (2.6)	4.01 (0.80)	7.50 (0.10)	20.5 (0.6)	5.03 (1.67)	27.6 (2.3)	0.103 (0.0865–0.126)	0.743 (0.575–1.02)	0.789 (0.478–1.23)	9.77 (7.37–13.5)
DHA	45.8 (2.2)	10.5 (2.3)	22.2 (2.5)	4.42 (0.77)	7.87 (0.43)	5.29 (0.15)	12.7 (2.4)	26.8 (1.7)	0.0650 (0.0583–0.0724)	0.192 (0.154–0.250)	1.10 (0.860–1.37)	9.02 (7.12–11.8)
IHA	24.5 (4.5)	9.41 (0.85)	21.8 (2.6)	0.589 (0.524)	9.20 (0.88)	29.2 (1.7)	3.75 (0.08)	36.7 (0.8)	0.132 (0.101–0.174)	1.26 (1.08–1.48)	0.665 (0.546–0.832)	14.8 (13.3–16.5)
1S101F	26.0 (2.0)	5.28 (3.01)	46.2 (14.5)	5.61 (1.08)	18.7 (0.6)	35.5 (0.7)	21.1 (2.6)	40.6 (0.3)	0.218 (0.185–0.261)	2.24 (1.47–4.49)	2.62 (2.04–3.38)	22.2 (15.8–36.6)
2S101F	49.8 (3.1)	4.30 (1.57)	60.8 (11.1)	6.23 (1.13)	16.2 (1.5)	24.3 (0.1)	18.7 (5.7)	37.2 (2.9)	0.108 (0.0905–0.129)	1.78 (1.35–2.62)	1.33 (0.880–1.87)	22.8 (17.1–31.9)
1R105F	37.9 (5.2)	6.13 (2.16)	26.7 (1.9)	5.16 (0.68)	16.9 (2.5)	20.2 (0.6)	8.46 (0.69)	39.0 (1.3)	0.162 (0.122–0.213)	1.16 (0.853–1.74)	0.964 (0.775–1.21)	19.2 (14.8–26.5)
1R109F	37.7 (2.1)	2.16 (1.94)	87.3 (15.7)	7.51 (1.79)	(n.a.)	(n.a.)	(n.a.)	(n.a.)	(n.a.)	(n.a.)	(n.a.)	(n.a.)
DFA	24.3 (1.3)	4.79 (1.31)	47.4 (13.2)	6.59 (0.87)	(n.m.)	(n.m.)	(n.m.)	(n.m.)	(n.a.)	(n.a.)	(n.a.)	(n.a.)
IFA	31.5 (1.1)	1.81 (1.73)	40.8 (9.7)	7.17 (0.77)	(n.a.)	(n.a.)	(n.a.)	(n.a.)	(n.a.)	(n.a.)	(n.a.)	(n.a.)
BFA	33.8 (1.5)	1.54 (2.08)	103 (7)	7.45 (1.63)	(n.a.)	(n.a.)	(n.a.)	(n.a.)	(n.a.)	(n.a.)	(n.a.)	(n.a.)
Inorganic Fe	8.8 <sup>b</sup>	0.38 <sup>b</sup>	37.2 <sup>b</sup>	4.79 <sup>b</sup>	(n.a.)	(n.a.)	(n.a.)	(n.a.)	(n.a.)	(n.a.)	(n.a.)	(n.a.)

(n.a.): not applicable; (n.m.): not measured.

<sup>a</sup> The values in parenthesis represent a standard deviation (SD) and the range estimated by taking the upper and lower limits for the SD of redox rate constants into account for the redox rate constants and  $[\text{Fe(II)}]_{\text{ss}}/[\text{Fe}]_{\text{T}}$ , respectively.

<sup>b</sup> Inorganic Fe(II) oxidation rate in the 2 mM  $\text{NaHCO}_3$  and 0.1 M NaCl from Pham and Waite (2008) [5].

Table 9: Kinetic model to explain iron redox transformation and ROS generation in the presence of exudate released by *M. Aeruginosa* (Wang et al. 2017)

**Table 1. Kinetic Model To Explain Iron Redox Transformation and ROS Generation in the Presence of Exudate Released by *M. Aeruginosa*<sup>a</sup>**

No.	Reaction	Rate Constant <sup>b</sup> (pH 4)	Published value <sup>b,c</sup> (pH 4)	Rate Constant <sup>b</sup> (pH 8)	Published value <sup>b,c</sup> (pH 8)
Dark Fe transformation					
1	Fe(III)L + Ex <sub>red</sub> → Fe(II)L + Ex <sub>ox</sub>	1.2 × 10 <sup>3</sup>	4 × 10 <sup>3</sup> (ref 12)	1.2 × 10 <sup>3</sup>	—
2	Ex <sub>red</sub> $\xrightarrow{\text{aging}}$ Ex <sub>ox</sub>	1 × 10 <sup>-4</sup> .s <sup>-1</sup>	—	1 × 10 <sup>-4</sup> .s <sup>-1</sup>	—
3	Fe(II)L + O <sub>2</sub> → Fe(III)L + O <sub>2</sub> <sup>•-</sup>	0.5	—	60	93 (ref 19)
4	Fe(II)L + H <sub>2</sub> O <sub>2</sub> → Fe(III)L + OH <sup>•</sup> + OH <sup>-</sup>	—	—	1.3 × 10 <sup>5</sup>	1.6 × 10 <sup>5</sup> (ref 19)
5	Fe(III)' + Fe(III)' $\xrightarrow{k_{p,hom}}$ 2AFO-L	—	—	1.6 × 10 <sup>7</sup>	1.6 × 10 <sup>7</sup> (ref 51)
6	Fe(III)' + AFO-L $\xrightarrow{k_{p,heter}}$ 2AFO-L	—	—	4 × 10 <sup>6</sup>	4 × 10 <sup>6</sup> (ref 52)
7	Fe(III)' + L → Fe(III)L	≥ 1 × 10 <sup>5d</sup>	—	0.1–5 × 10 <sup>6d</sup>	2.5 × 10 <sup>6</sup> (ref 48)
8	Fe(II)' + L → Fe(II)L	≥ 5 × 10 <sup>3d</sup>	—	≥ 1 × 10 <sup>5d</sup>	12 g <sup>-1</sup> .L.s <sup>-1</sup> (ref 50)
9	AFO-L $\xrightarrow{k_d}$ Fe(III)'	—	—	2.3 × 10 <sup>-4</sup> .s <sup>-1</sup>	2.3 × 10 <sup>-4</sup> .s <sup>-1e</sup> (ref 47)
10	Fe(III)L → Fe(III)' + L	≤ 3 × 10 <sup>-3</sup> s <sup>-1</sup>	—	≤ 1 × 10 <sup>-3</sup> s <sup>-1</sup>	9 × 10 <sup>-5</sup> .s <sup>-1</sup> (ref 50)
Light-mediated O <sub>2</sub> <sup>•-</sup> and H <sub>2</sub> O <sub>2</sub> generation and consumption					
11	Q $\xrightarrow{hv}$ Q <sup>*</sup> $\xrightarrow{O_2}$ O <sub>2</sub> <sup>•-</sup>	9 × 10 <sup>-11</sup> M.s <sup>-1</sup>	—	4 × 10 <sup>-10</sup> M.s <sup>-1</sup>	—
12	O <sub>2</sub> <sup>•-</sup> $\xrightarrow{Ex}$ 1/2 H <sub>2</sub> O <sub>2</sub> + 1/2 O <sub>2</sub>	0.12 s <sup>-1</sup>	1.1 × 10 <sup>7</sup> (ref 15)	0.12 s <sup>-1</sup>	0.12 s <sup>-1</sup> (ref 39)
13	H <sub>2</sub> O <sub>2</sub> $\xrightarrow{Ex}$ O <sub>2</sub> /H <sub>2</sub> O	4 × 10 <sup>-4</sup> .s <sup>-1f</sup>	—	—	—
14	Ex $\xrightarrow{hv}$ R <sup>*</sup>	—	—	1.5 × 10 <sup>-10</sup> M.s <sup>-1</sup>	1.7 × 10 <sup>-9</sup> M.s <sup>-1g</sup> (ref 38)
15	R <sup>*</sup> + O <sub>2</sub> <sup>•-</sup> → R <sup>-</sup> + O <sub>2</sub>	—	—	1 × 10 <sup>5</sup>	1 × 10 <sup>5</sup> (ref 38)
Light-mediated Fe(III) reduction					
16	Fe(III)L $\xrightarrow{hv}$ Fe(II)' + L <sub>ox</sub>	3 × 10 <sup>-3</sup> .s <sup>-1</sup>	7.5 × 10 <sup>-3</sup> .s <sup>-1</sup> (ref 49)	3 × 10 <sup>-3</sup> .s <sup>-1</sup>	—
17	AFO-L $\xrightarrow{hv}$ Fe(II)' + OH <sup>•</sup>	—	—	1.2 × 10 <sup>-4</sup> .s <sup>-1h</sup>	—
18	Fe(III)' $\xrightarrow{hv}$ Fe(II)'	—	—	5 × 10 <sup>-4</sup> .s <sup>-1i</sup>	5 × 10 <sup>-4</sup> .s <sup>-1i</sup>
19	Fe(III)L + O <sub>2</sub> <sup>•-</sup> → Fe(II)L + O <sub>2</sub>	—	—	(3–100) × 10 <sup>4</sup>	(2.5–5.6) × 10 <sup>4</sup> (ref 15)
20	Fe(III)' + O <sub>2</sub> <sup>•-</sup> → Fe(II)' + O <sub>2</sub>	—	—	1.5 × 10 <sup>8</sup>	1.5 × 10 <sup>8</sup> (ref 23)
Light-mediated Fe(II) oxidation					
21	Fe(II)L + O <sub>2</sub> <sup>•-</sup> → Fe(III)L + H <sub>2</sub> O <sub>2</sub>	—	—	2 × 10 <sup>6</sup>	0.43–2.3 × 10 <sup>6</sup> (ref 5)

<sup>a</sup>AFO-L: exudate-coated iron oxyhydroxide, Fe(III)L and Fe(II)L: exudate-complexed Fe(III) and Fe(II), respectively. Fe(III)' and Fe(II)': inorganic Fe(III) and Fe(II), respectively. L: Fe-binding ligand in exudate. Ex<sub>red</sub>: Fe(III)-reducing moieties intrinsically present in the exudate. Ex: bulk organic moieties in the exudate involved in O<sub>2</sub><sup>•-</sup> and R<sup>\*</sup> generation. R<sup>\*</sup>: photogenerated oxidizing organic moieties. <sup>b</sup>Rate constants listed are in units of M<sup>-1</sup> s<sup>-1</sup> unless stated otherwise <sup>c</sup>Published values of the rate constant shown here are the values reported in the SRFA system unless stated otherwise. <sup>d</sup>Based on L concentration of 65.6 nmoles.mg<sup>-1</sup> C of exudate as reported to be the case for SRFA. <sup>e</sup>Reported for 1 min aged iron oxyhydroxide. <sup>f</sup>Calculated based on the measured H<sub>2</sub>O<sub>2</sub> decay rate in exudate solution at pH 4. <sup>g</sup>Calculated using the reported bulk organic concentration involved in R<sup>\*</sup> generation in the SRFA solution. <sup>h</sup>Calculated based on the measured Fe(II) formation rate on Fe(III) reduction in an exudate-free medium at pH 8. <sup>i</sup>Calculated based on the measured Fe(II) formation rate on Fe(III) reduction in an exudate-free medium at pH 4.